Statistical Modeling of Intelligent Transportation Systems Communication Channels

TARIKUL ISLAM

Master of Science Thesis

Wireless and Mobile Communications Group

Department of Telecommunications

Faculty of Electrical Engineering, Mathematics and Computer Science

Delft University of Technology

TU Delft Delft University of Technology

TNO innovation for life

Statistical Modeling of Intelligent Transportation Systems Communication Channels

Master of Science Thesis

For the degree of Master of Science in
Wireless and Mobile Communications
at Department of Telecommunications
at Delft University of Technology

Tarikul Islam

14.05.2013

Faculty of Electrical Engineering, Mathematics and Computer Science
Delft University of Technology
Delft, The Netherlands

Delft University of Technology
Department of
Telecommunications

The undersigned hereby certify that they have read and recommend to the Faculty of Electrical Engineering, Mathematics and Computer Science for acceptance a thesis entitled

Statistical Modeling of Intelligent Transportation Systems Communication Channels

by

Tarikul Islam

in partial fulfillment of the requirements for the degree of

Master of Science.

Dated: 14.05.2013

Supervisors:

dr. Ertan Onur (Assistant Professor, TU Delft)

dr. Bert Boltjes (TNO - Modelling, Simulation and Gaming)

Prof. K.G. Langendoen (Professor, TU Delft)

Readers:

Prof. dr. B.J. Kooij (Professor, TU Delft)

Yongchang Hu (PhD Student, TU Delft)

Abstract

Intelligent Transportation Systems (ITS) is becoming an important paradigm, because of its ability to enhance safety and to mitigate congestion on road traffic scenarios. Realizing the fact that data collection scheme from in-situ test beds for large number of vehicles is always expensive and time consuming, before being employed in large scale, such safety critical system should be tested narrowing down the gap between real circumstances and analytical models in a simulation platform. It is evident that underlying radio wave propagation models can comprise the validity of large scale vehicular network simulation results. Vehicle to Vehicle (V2V) channels have higher dynamics due to rapidly varying topologies and environments which have significant impact on performance study of upper layer protocols and applications. In spite of the fact that few measurement based empirical channel models are present in the literature, they are not tested for large scale vehicular networks. Recently, IEEE has approved IEEE 802.11p which is the standard for Dedicated Short Range Communications (DSRC). During this MSc thesis, required amendment to the TNO's in-house OPNET based 802.11p node model was made to meet the IEEE standard. To the best of author's knowledge large scale simulation study of 802.11p nodes with realistic channel model is not present in the literature. Three different vehicular scenarios (i.e. suburban, highway, rural) were simulated with hundreds of IEEE 802.11p nodes in OPNET. For bringing down gap between real life behaviors of wireless channels in V2V communication a realistic Nakagami-m fading channel was developed to replace the standard OPNET propagation model. For the sake of implementing varying speed and separation distance, power spectrum and fading parameter-m were defined as function of velocity and separation distance respectively. Statistics were collected for large scale vehicular scenarios to evaluate performance of physical and higher layers. Retrieved scenario based results were compared with empirical channel models which showed fine resemblance between the mentioned models. Primarily, it was found that all the vehicles within the standard requirement for DSRC range of 1 kilometer may not receive packets. Finally, three different scenarios were collated which deduced that the multipath fading is more deciding factor for communication quality in contrast to the Doppler effect.

Acknowledgements

First of all I would like to thank Dr. Bert Boltjes for his continuous support and supervision during carrying out this graduation project at Netherlands Organization for Applied Scientific Research (TNO). Time to time I have found him as a great source of motivation. Through out the whole process he has supported this research with his technical expertise and organizational credentials. He has also allowed me to work independently when it was required. Overall, it was pleasure to work with him in the same team. Without his support and guidance this work could not be accomplished.

I would also like to offer sincere gratitude to Dr. Ertan Onur and Yongchang Hu. Their guidance and assistance to set the research goals and to attain feasible results were the key learning points of this assignment. These skills will be always with me to achieve greater success in the future research career waiting ahead of me. Special thanks to Dr. Onur for his contributions while writing the publication. I would also like to convey my appreciation to Yongchang as he was always ready to help when I found it difficult.

I would like to thank Prof. Dr. K.G.Langendoen and Prof. Dr. B.J.Kooij for their courteous agreement to become thesis committee members and to spend their time to read the thesis.

Special thanks to Network Technology department, TNO for their financial assistance to carry out the research and to present the publication in Czech Republic. I would like to appreciate feedbacks and efforts from Martijn van Noort, Dr. J.F.C.M de Jongh, and Jaap van den Oever of TNO. They helped me to define different vehicular scenarios and physical layer parameters.

Last but not the least, I would like to express my dedication to my parents, family members, and friends. Without their support my studies in Delft University of Technology would have remained outreached.

Delft, The Netherlands — Tarikul Islam

Publications

1. **IEEE conference publication**

   (a) T. Islam, B. Boltjes, Y. Hu, E. Onur, J.F.C.M de Jongh, "Realistic Simulation of IEEE 802.11p Channel in Mobile Vehicle to Vehicle Communication," in *13th International Conference on Microwave Techniques (COMITE)*, Pardubice, Czech Republic, April 17-18, 2013.

2. **Papers to be submitted**

   (a) B. Boltjes, T. Islam,"Modeling and Simulation of WLAN 802.11p for Vehicle to Vehicle Communication in Military Deployments and Scenarios," in *MILCOM*, IEEE, San Diego, USA, 2013.

   (b) T. Islam, B. Boltjes, E. Onur, Y. Hu, "OPNET Pipeline Stage Modeling for Vehicular Network and Evaluation Using IEEE 802.11p Nodes," in *Proceedings: Intelligent Transportation Systems*, IEEE, 2013.

Table of Contents

List of Figures

List of Tables

Chapter 1

Introduction

In recent years, required developments for the wireless vehicular network are being realized as it can contribute effectively to look-ahead vehicle collision avoidance, alleviate congestion, lane change, and construction site warning. An IEEE task group has approved the IEEE 802.11p standard to enhance 802.11 capabilities to support Intelligent Transportation Systems (ITS). The proposed standard will be used as a base element of Dedicated Short Range Communications (DSRC) for vehicular scenarios. For harmonized use, in the year of 2008 Commission of European Communities (CEC) assigned 5875 MHz to 5905 MHz frequency spectrum for ITS [7]. However, foreseeable real time and safety critical applications demand reliable channel models tested with large number of vehicles before being implemented in road traffic scenarios. This thesis contributes a novel simulation study and presents a realistic channel model tested with a large number of IEEE 802.11p nodes.

Empirical studies deploying a large number of vehicles on the roads are expensive, time consuming, and require permission from transport regulatory authority. Furthermore, an empirical model derived measuring one vehicular scenario (e.g. highway) may not become pertinent universally (e.g. suburban, urban, rural). Question arises, how many scenarios can be measured using a large number of vehicles to collect data? Considering the mentioned drawbacks of the in-situ measurements simulation could be the answer. However, to a great extend the accuracy of large scale simulation results of Vehicle to Vehicle (V2V) communication depends upon underlying propagation channels as V2V channels have strong influence over coverage, reliability, and real time capabilities [22]. The research community has presented several contributions on vehicular channel models using both measurements and simulations. Though empirical models for small scale networks were studied in several papers, validity of those models for large scale networks are not tested yet. All the measurements in those studies were taken using one transmitter and one receiver. On the other hand, most of the simulation studies were based on overly optimistic free space or two-ray propagation model. As a result, the validity of the results still remained under questions. The impact of buildings

and the distance attenuation on received signals were presented in [38] without stating the effects of multipath propagation. Position based message forwarding strategy was used in [39], where it was assumed that each vehicle will periodically disseminate status information. However, a DSRC station uses the demand beacons that need not be periodically repeated [2]. For the sake of achieving a faster simulation, hybrid method was used for a large number of vehicles in [40]. But both in [39] and [40], Nakagami fading model was implemented for fixed fading parameters-m and a constant average velocity. Since, V2V propagation environment changes with vehicle mobility, all the channels will not necessarily suffer the same fading. In [41], the SHIFT simulator was used for a large number of IEEE 802.11a radios to evaluate V2V safety messaging. For simulation of Medium Access Control (MAC) and higher layers an error model approach was presented in [42] and validated using Wireless Access Radio Protocol 2 (WARP2) simulator. A two-ray interference model was presented in [43] to replace the simplified two-ray model. Computationally an inexpensive radio shadowing model was studied in [44]. All these contributions were again based on free space or two-ray propagation model that does not consider multipath propagation and based on an optimistic assumption of real life scenarios.

1-1 Research challenges

Overall, there is an persisting disagreement between the presented vehicular channel models and what the channels actually are for vehicle to vehicle communication. Following the stated absence, the goal of this research was to bring out more realistic channel models for different vehicular scenarios. It was of greater concern how varying propagation environment due to higher dynamics and the rapidly varying topology of the network could be analytically defined in the model. In contrast to other mobile network technologies, vehicular nodes have higher mobility. As a result, V2V channel models must characterize transmitter (Tx) and receiver (Rx) velocities to predict signal fading and communication quality. This was particularly challenging to delineate channel conditions due to the impact of velocities for each of the communicating Tx-Rx pairs.

1-2 Methodology

Like most of the existing network simulators OPNET does not have IEEE 802.11p communication and stochastic channel models (e.g. Nakagami). Netherlands Organization for Applied Scientific Research (TNO) has developed an IEEE 802.11p node model in OPNET for performance evaluation of ITS. During this graduation project further improvements were made to the node model to meet recently published amendment of the standard. The developed node model was used in a large scale for this simulation study.

Universal deterministic modeling of wireless channels for V2V communications is almost impossible. As a result, the most accepted stochastic channel model the Nakagami-

m fading channel was programmed to replace the OPNET default free space propagation model. The Nakagami-m parameter was varied in relation to the separation distance between Tx and Rx to address varying multipath anomalies with propagation environments. Since, both the Tx and Rx are in motion, to calculate power spectrum the autocorrelation function presented in [32] was used in the simulation model to address varying velocity attributes.

One of the major objectives of this assignment was to define different vehicular scenarios. After literature survey consistent parameters to characterize suburban, highway, and rural scenarios were found. Analysis in the field showed, Dual Slope Piecewise Linear (DSPL) path loss model fits better with the measurements. Moreover, only for the DSPL model specific empirical parameter values to define different vehicular scenarios were found in the study. The measured parameters given in [20] and [21] were used to delineate realistic large scale path loss for the respective vehicular scenarios.

Mobility is the inherent characteristic which differentiate vehicular network from infrastructure networks. As a result, appropriate trajectory assignment is very important for the proof-of-concepts. In this study, vehicle velocity, average vehicle density, and traffic condition parameters for the corresponding scenarios were chosen by consulting experts in the field.

Hundreds of vehicles with specific trajectory settings were simulated to retrieve statistics. The results were then compared with other propagation models (i.e., free space, two-ray, and empirical). The comparison showed the results of the proposed realistic channel model resembled with that of the empirical model. In contrary, considerable differences between the simulation results of overly simplified channel models and the proposed model were observed.

1-3 Contributions

This research presents a novel simulation study of OPNET based large scale IEEE 802.11p network. Unlike most of the efforts found in the literature realistic channel models were used in the simulation. While few empirical studies were found to characterize V2V communication channel models, pertinence of those measurement based models for large scale networks were not reported. This study examined validity of the mentioned empirical models for large scale use case.

Vehicular scenarios were defined as suburban, high way, and rural scenarios. However, the comparisons among the scenarios were rarely studied for better understanding of the propagation anomalies in different scenarios. In this research, all the three different scenarios were bring forth to the same platform and were analyzed and compared.

For more accurate definition of V2V communication channel models, it is required to properly address vehicular network attributes in the model. With mobility of the nodes not only the topology or the Tx-Rx separation distance is changing but also the surrounding propagation environment is varying. As a result, presence of multipath scatterers are also increasing or decreasing. To define this particular problem a novel

analytical relationship was derived based on test bed data. This model can be used to vary Nakagami fading parameter-m with distance. Hence, with varying distance the signal fading will also change.

The most important characteristic of vehicular network Tx and Rx velocities were included in the calculation of fading envelope. Though the implemented model was presented in [32] quite long time ago, use of that model in the Nakagami-m fading channel was not found in the literature. Overall, the proposed realistic channel model is an unique contribution which includes all the features to be used in V2V communication.

As obtained results will be fed to Java ITS modeler currently being developed by TNO, the performance of newly developed 802.11p node model was studied using the proposed channel model. Effort was given to achieve realistic simulation results by creating scenarios that possess real life attributes (e.g. speed limit in the suburban scenario) corresponding to the scenarios. Furthermore, it was found that using overly optimistic channel models can substantially alter the results which are unusable for implementation in real life safety critical systems.

1-4 Organization

Rest of the thesis is organized as follows, in Chapter 2 the background information related to the 802.11p standard, modeling concepts in OPNET, and state of the art measurement based vehicular channel models for different scenarios are presented. Chapter 3 outlines required elements to construct an OPNET based vehicular scenario. The developed 802.11p node model is also discussed in details in that chapter. Chapter 4 presents different aspects of multipath propagation in vehicular communications and the proposed realistic channel model. Chapter 5 describes implementations of the three different scenarios in OPNET and simulation results obtained using the proposed Nakagami channel model for the respective scenarios. Finally, Chapter 6 concludes this thesis providing a clear picture of the contributions, and the future works.

Chapter 2

Background

Intelligent Transportation Systems (ITS) is an innovative way of vehicular traffic management. Utilizing synergistic technologies and system engineering concepts major goal is to increase safety and reduce congestion on road traffic scenarios. Different applications are being studied to make the journeys more pleasant and efficient. Wireless communication module between Vehicle to Infrastructure (V2I) and Vehicle to Vehicle (V2V) is the key element to enable those services. This chapter illustrates background information relevant to this research assignment. At the beginning, ITS standards for Physical Layer (PHY) and Medium Access Control (MAC) layer are discussed. In the following section, appropriate channel modeling concepts specific to the different vehicular scenarios are outlined.

2-1 Intelligent Transportation Systems (ITS) standards

In May 2010, IEEE Task Group approved IEEE 802.11p with 95 percent affirmative votes and without any comments which was to enhance 802.11 capabilities to support ITS. This augmentation to support ITS applications also been called Wireless Access in Vehicular Environments (WAVE). The WAVE devices can be classified as Road Side Unit (RSU) and On Board Unit (OBU). Possible ways of communications between mentioned devices are V2I and V2V. Direct V2V communication reduces message delivery latency which is a key factor for distributing safety messages. Major communication system parameters of WAVE combine IEEE 802.11a PHY and 802.11 Carrier Sense Multiple Access Collision Avoidance (CSMA/CA) MAC protocols [1]. The proposed standard will be used as a base element of Dedicated Short Range Communications (DSRC) for short and medium range wireless communications in vehicular scenario. 5.9 GHz band was allocated for ITS in Europe and USA. Foreseeable applications of ITS are traffic management and congestion avoidance to reduce overall fuel consumption, dissemination of traffic safety messages, and toll collection. In the following subsections details

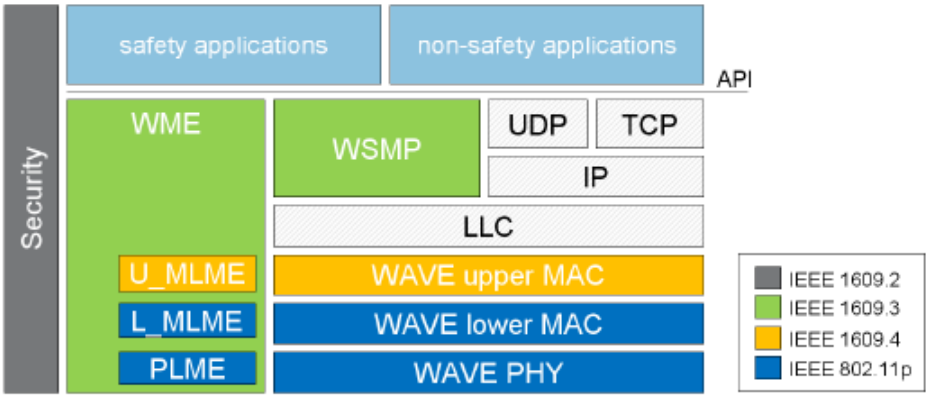

Figure 2-1: WAVE Standards.

architecture of physical and MAC layer proposed by IEEE and European Telecommunications Standards Institute (ETSI) will be discussed.

2-1-1 WAVE protocol stack

For a non stationary environment and decentralized spreading of network traffic, 802.11p defines required functions and services to be implemented in WAVE stations. On the contrary, in traditional infrastructure IEEE 802.11 any arbitrary mobile node needs to join in a Basic Service Set (BSS) before retrieving Access Point (AP) resources and services [2]. Furthermore, IEEE 802.11p should characterize WAVE signaling techniques and interface functions to attain optimum overall performance. We observe in Fig. 2-1 that IEEE 802.11p WAVE performs only a part of the task of DSRC in PHY and MAC layer. IEEE 1609.4 enables upper layer data transfer operation across multiple channels without necessity of any prior knowledge of PHY parameters, and performs multichannel routing and switching for different scenarios [3]. Whereas, IEEE 1609.3 is responsible for layer-3 and layer-4 tasks of the Open System Interconnect (OSI) communication stack. This standard offers addressing and data delivery services within a WAVE system, providing multiple higher layer entities access to WAVE communication services [4]. Upper layer services may consist of in-vehicle applications for safety and convenience to the end user. As many DSRC WAVE applications are safety critical, IEEE 1609.2 provides security against potential threats like eavesdropping, spoofing, alteration, and replay. Safety services of WAVE management messages and application messages are described by this standard [5]. Please refer to the mentioned citations for details information about these standards.

2-1-2 IEEE 802.11p physical layer (PHY)

IEEE 802.11p PHY standard is adapted from IEEE 802.11a which was originally standardized for relatively stationary indoor environments. Consequently, vehicular scenarios face very harsh signal propagation environment due to the fact that both transmitter and receiver are in motion, and there are both stationary and mobile scatterers present to play a role in overall degradation of signal strength. Furthermore, this

Table 2-1: Nominal carrier frequency allocation by ETSI/IEEE.

Channel number	Channel type	Spectrum	Merge option
Channel 1	service (non-safety)	5855 MHz - 5865 MHz	20MHz Channel
Channel 2	service (non-safety)	5865 MHz - 5875MHz	
Channel 3	service (safety)	5875 MHz - 5885MHz	30MHz Channel
Channel 4	control channel	5885 MHz - 5895MHz	
Channel 5	service (safety)	5895 MHz - 5905MHz	
Channel 6	service (safety)	5905 MHz - 5915MHz	20MHz Channel
Channel 7	service (safety)	5915 MHz - 5925MHz	

DSRC network's primary requirements are reliability and robustness as risk of human life is directly involved with the applications. To meet the requirements of real time safety applications, WAVE must possess low latency for disseminating safety critical messages, high throughput, scalability, and high fidelity against different propagation environments [6]. To enhance public safety, in 1999 United States Federal Communication Commission allocated 75 MHz bandwidth of DSRC at 5.9 GHz frequency for V2V and V2I communications. Commission of European Communities has assigned 5875 MHz to 5905 MHz frequency spectrum for ITS [7]. In Table. 2-1, the nominal carrier frequency allocation defined by ETSI is presented which was disclosed in its Harmonized Standard EN 302 571. The designated 75 MHz bandwidth is divided into seven 10 MHz channels. Channels 1, 2, 3, 5, 6, 7 are service channels, and channel 4 is assigned as control channel which can be only used for system control, service announcement, and low latency service messages. IEEE has defined identical channel allocation for DSRC. To preserve scalability for higher throughput, ETSI has left the option to merge channels 1 and 2 and optionally used as a channel with a maximum channel bandwidth of up to 20 MHz. The same is applicable for channels 7 and 9. These two channels can be combined and to be used as a channel with a maximum channel bandwidth up to 20 MHz. Similarly, channels 4, 5 and 6 can optionally be used as a channel with a maximum combined channel bandwidth of 30 MHz. WAVE data rate can be varied between 3 to 27 Mbps on 10 MHz channel depending on the type of modulation scheme applied. Detail comparisons of IEEE 802.11p and IEEE 802.11a physical parameters are presented in Table. 2-2. To achieve required robustness against fading the bandwidth is reduced to 10 MHz and symbol length is doubled. This is effectively achieved by halving the clock rate. Beside these parameters, Adjacent Channel Rejection (ACR) and the Spectrum Emission Mask (SEM) for WAVE also changed compared to 802.11 [9].

2-1-3 IEEE 802.11p MAC layer

Physical layer properties of WAVE are rapidly changing and very short duration of communications exchanges are mandatory for safety critical and applications. As a consequence, association and authentication must be completed in time frames much shorter than that of infrastructure or ad-hoc IEEE 802.11 networks [11]. Details about the modifications in PHY layer have already been discussed in the previous section. IEEE 802.11e amendment defines MAC sublayer procedures to support local area net-

Table 2-2: Comparable physical parameter set for IEEE 802.11a and IEEE 802.11p.

Parameters	802.11a Standard	802.11p Standard	Adaptation
Bit rate (Mbps)	6, 9, 12, 18, 24, 36, 48, 54	3, 4.5, 6, 9, 12, 18, 24, 27	Halved
Modulation Scheme	BPSK, QPSK, 16QAM, 64QAM	BPSK, QPSK, 16QAM, 64QAM	Remains same
Code rate	1/2, 2/3, 3/4	1/2, 2/3, 3/4	Remains same
Number of OFDM subcarriers	52	52	Remains same
FFT period	3.2μs	6.4μs	Doubled
Symbol duration	4μs	8μs	Doubled
Guard time	0.8μs	1.6μs	Doubled
Preamble duration	16μs	32μs	Doubled
Subcarrier spacing	0.3125 MHz	0.15625 MHz	Halved

work Local Area Network (LAN) applications with Quality of Service (QoS) requirements, including the transport of voice, audio, and video over IEEE 802.11 wireless Wireless Local Area Network (WLAN)s [10]. WAVE devices use the Enhanced Distributed Channel Access (EDCA) MAC protocol to compete for the transmission medium which was defined in the 2007 version of the IEEE 802.11 specification. In the following subsections EDCA and IEEE 1609.4 standard will be discussed in detail.

2-1-3-1 Enhanced Distributed Channel Access (EDCA)

EDCA uses CSMA/CA access method which means all the mobile nodes are bound to sense the channel to reveal availability of the channel resources. The primary reason for EDCA is to assure QoS. If the channel is free for an Arbitration Inter-frame Space (AIFS) the corresponding node can transmit packets immediately. AIFS is the minimum amount of time a node must sense the channel and distinct values are solely dependent upon Access Categories (AC) defined by the IEEE standard. If the channel is busy for an AIFS or becomes busy while waiting for an AIFS the corresponding radio must perform a back-off procedure. Safety related urgent information are given highest priority which could be present in RSU. Few examples of urgent situations are, accidents, emergency vehicle routing, malfunctioning vehicle hardware, slippery or damaged roads, obstacles, abnormal driving behaviour (e.g. vehicle speeding over the specific limit) and broken or missing traffic signs [23]. Then priority should be give to the vehicles are to announce their presence to other vehicles in the vicinity within the range of communication. This is particularly useful when visual detection is not possible due to turning roads, terrain, or hazardous weather conditions. Immediate lower priority should be assigned to messages which contain information about necessity of help because of collision with obstacles, shortage of fuel, or broken down but do not posses any dangerous threat to other vehicles. Lastly, lowest priority can be assigned to non-safety related messages over service channels. MAC layer in WAVE is equivalent to the IEEE 802.11e EDCA QoS extension [24]. As a result, application messages are divided into different AC. Each channel is divided into four different AC. Important EDCA AC parameters for WAVE networks are presented in Table. 2-3. In the table, we can see higher priority traffic has shorter Contention Window (CW) and shorter AIFS. The frames for traffic belonging to different ACs are placed in different queues, which are then served based on internal contention procedure. The explained procedure is presented in Fig. 2-2.

Table 2-3: Control channel default EDCA parameters.

Access Category	CWmin [AC]	CWmax [AC]	AIFSN [AC]	Max TXOP
Background (AC_BK)	aCWmin	aCWmax	9	0
Best Effort (AC_BE)	(aCWmin + 1)/2 -1	aCWmax	6	0
Video (AC_VI)	(aCWmin + 1)/4 -1	aCWmin	3	3.008ms
Voice (AC_VO)	(aCWmin + 1)/4 -1	(aCWmin + 1)/2 -1	2	1.504ms

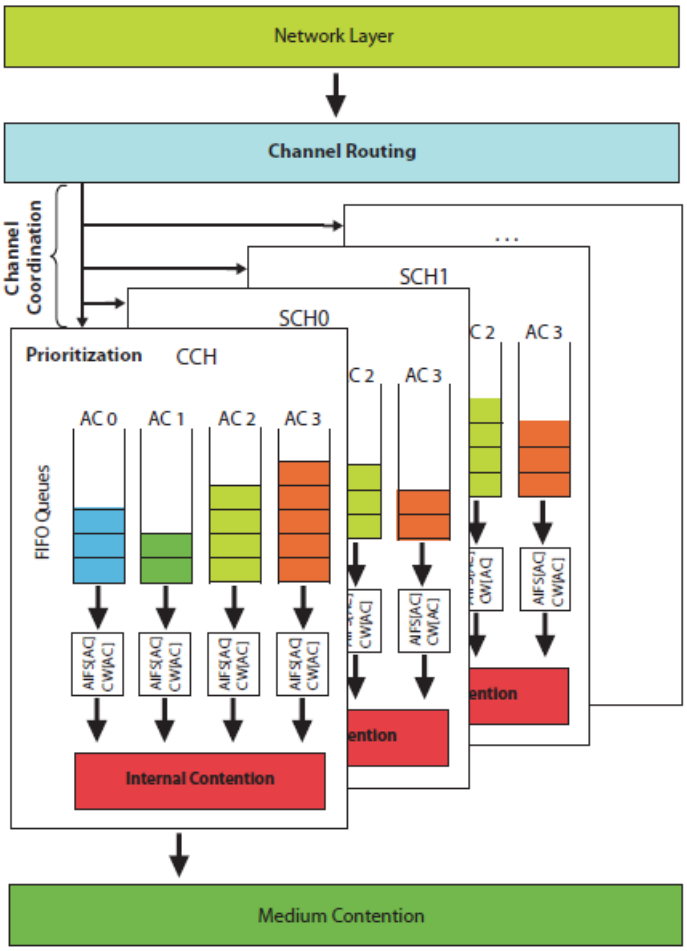

Figure 2-2: IEEE 802.11p traffic prioritization with different Access Categories.

Table 2-4: Access Category default values for EDCA.

Access Category	CWmin [AC]	CWmax [AC]	AIFSN [AC]
AC_BK	15	1023	9
AC_BE	7	225	6
AC_VI	3	7	3
AC_VO	3	7	2

During Transmit Opportunity (TXOP) time a wireless device can send as many frames as possible till the maximum possible duration of TXOP. Larger frames can be segmented to smaller ones to fit in TXOP. IEEE has addressed these very important QoS parameters as follows [3]:

- **Arbitration inter-frame space (AIFS):** The minimum time interval between the wireless medium becoming idle and the start of transmission of a frame.
- **Contention window (CW):** An interval from which a random number is drawn to implement the random transmit back-off mechanism.
- **Transmit opportunity (TXOP) limit:**The maximum time duration (in milliseconds) for which a station can transmit after obtaining a TXOP. If the TXOP limit is 0, the transmit opportunity only permits the transmission of a single MAC Protocol Data Unit (MPDU).

EDCA can differentiate between beacons using these channel access parameters. The default parameter values for IEEE 802.11p are given in Table. 2-4 which are calculated based on the typical values for Orthogonal Frequency Division Multiplexing (OFDM), when aCWmin = 15 and aCWmax = 1023. It could be interpreted from the table that lower CW values ensure access for higher AC traffics over lower AC. The queues for ACs presented in Fig. 2-2 have different timer settings for different channels. Four ACs have different AIFS and back off time depending on whether the mobile node is switched to control channel or service channel. To portray internal contention procedure in [25], authors have presented Fig. 2-3 which is easy to interpret. In the figure we can see AC3 (Voice (AC_VO)) has highest priority. This is to give the voice communication higher priority to be transmitted with low latency or delay. AC2 (Video (AC_VI)) has similar AIFS and back-off time as both voice and video are delay critical. Where as, AC1 (Best Effort (AC_BE)) and AC0 (Background (AC_BK)) have relatively lower priority compared to voice and video as a result they have higher AIFS and back-off time.

2-1-3-2 IEEE 1609.4 standard

The IEEE 1609.4 standard enables WAVE to the coexistence of safety related and non-safety related applications. Number of channels were defined each of which should be used for different applications with different characteristics. In Fig. 2-4, we can see channel types and their specific applications [25]. It is noticeable from the figure that

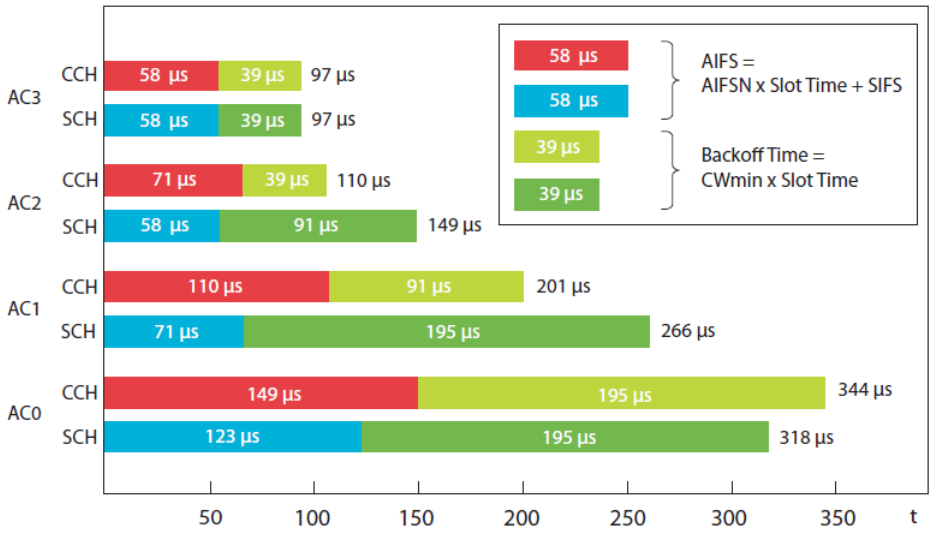

Figure 2-3: AIFS and Back-off time for IEEE 802.11p EDCA.

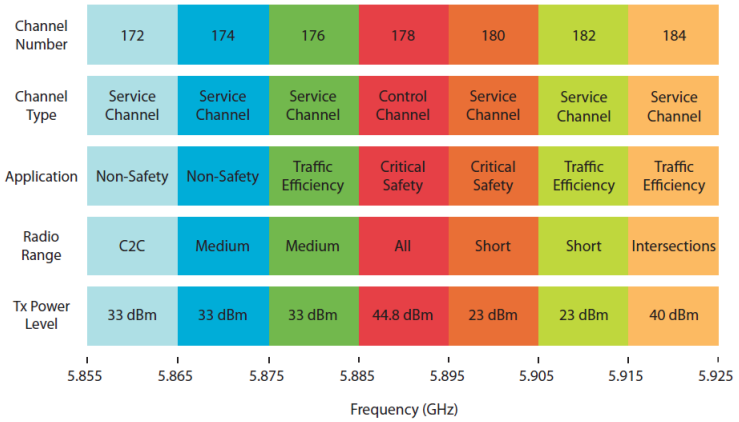

Figure 2-4: Different channels for multichannel operation with specified transmit power.

depending on the application and range different frequency spectrum was allocated. Transmit power is also shown in the figure. For DSRC applications the range of allowable transmit power is 23 dBm to 44.8 dBm. The control channel has highest transmit power as safety critical information dissemination is operated over the control channel. This is to attain optimum range within which mobile vehicles will receive safety messages. In 1609.4 scheme each vehicle periodically switches between Control Channel Interval (CCHI) and Service Channel Interval (SCHI). The default length of time interval is 50ms. During the period of CCHI vehicles are only allowed to switched on to control channel and can transmit routine HELLO messages or event driven safety messages [26]. WAVE service advertisements are also announced during CCHI to publicize services in the upcoming SCHI. During service channel intervals vehicles can switch to remaining six service channels to use various non-safety applications.

2-2 Hierarchical modeling in OPNET

OPNET provides an easy to use graphical user interface and way of hierarchical modeling of complex networks. Each network model consists of several nodes, links, and subnets. Several process models form a node model. Whereas, original source code lays in the process models. In Fig. 2-5, the arrangement of a network model retrieved from [27] is presented. In the figure, we can see different modeling editors where a scenario editor lays on top of the other lower modeling layers. The scenario editor specifies the location and span of the network. While creating the project, startup wizard can be used to define different initial network topology or creating an empty scenario. Span of the network can be chosen from network scales of world, enterprise, campus, office, logical, or from map. There are different units to characterize the network extend (e.g. degrees, kilometers, miles, etc.). Different technologies and vendor specific systems can also be chosen from the start up wizard. Few of the built in technologies are available with the Modeler models of equipment of Alcatel Lucent, Cisco, Cabletron, etc. Different server models also exist in the OPNET model family. Some of them are to mention Dell, HP, Intel, IBM, and Sun. Furthermore, OPNET Modeler comprises wide variety of models for simulation study of wireless networks. In built WLAN, Universal Mobile Telecommunications System (UMTS), zigbee, and Long-Term Evolution (LTE) model families allow users to directly implement the concepts just by drag and drop in the simulation scenarios. As a result, without prior knowledge of lower modeling layers users can stay focused with specific modeling task or analyzing system performance. Each model suite includes several node models. In the figure, we can see several nodes can be accessed from project editor. The node editor outlines internal architecture of each node where several node models are connected by wire or packet stream. The node editor and process editor will be discussed in subsequent sections with IEEE 802.11p node model.

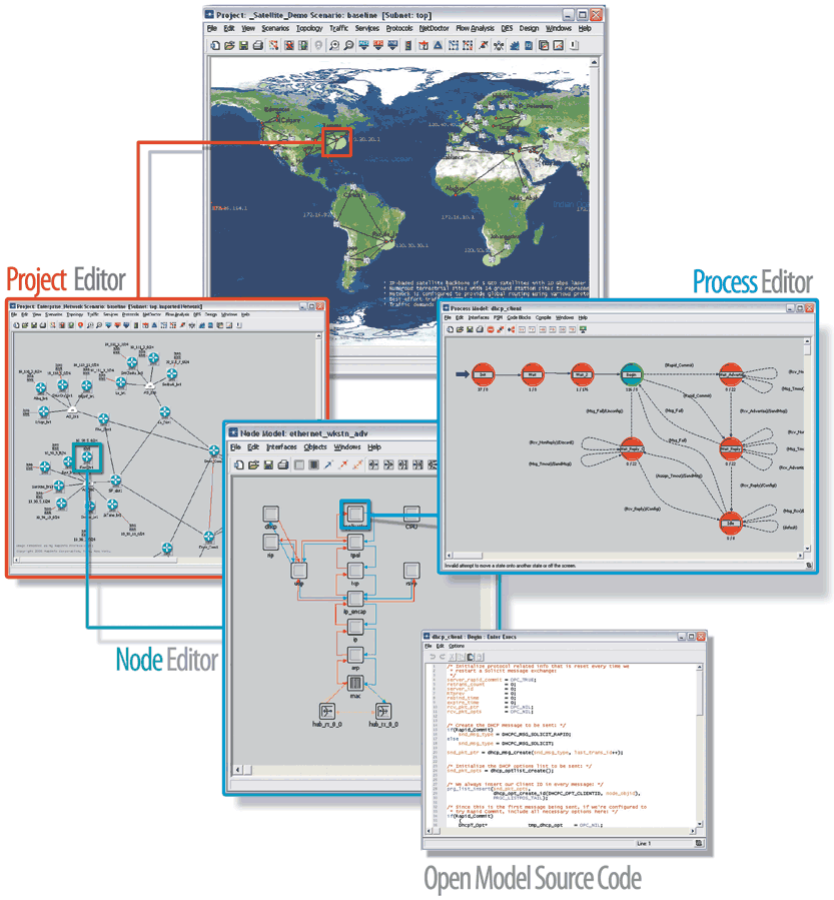

Figure 2-5: Series of hierarchical editors for OPNET modeling concept.

2-2-1 OPNET wireless LAN model suite

In this section OPNET WLAN node models will be discussed in detail as IEEE 802.11p node model was developed based on WLAN station of the Modeler. The in built WLAN node models are as follows,

Application configuration: allows users to define the required applications and parameters for those applications. For example, Hypertext Transfer Protocol (HTTP) heavy traffic browsing.

Profile configuration: provides opportunity to specify different profiles depending on different user groups. For example, in a office, programmers (e.g. download softwares) and management (e.g. email) have different preferences for network traffics. Each of the profile must have one application configuration. This provides a way of setting up more scalable networks for simulation.

Receiver group configuration: this node model can be used to delineate number of receivers which will receive the transmitted message. During simulation of

vehicular scenarios, receivers within the range of 1 km of the transmitter was considered as potential candidate for receiving the message.

Task specification: this node model could be used to specify a task depending on the application. An example would be authentication of a client before allowing access to a particular application.

Wireless Local Area Network Server (WLANS): could be chosen as mobile node or fixed node. For mobile server nodes, different trajectories can be assigned so that the WLANSs follow a desired path during simulation. In the node attributes menu Ad-Hoc routing protocols like Ad-Hoc Ad-Hoc On Demand Distance Vector routing (AODV) protocol, Dynamic Source Routing (DSR) protocol, Geographic Routing Protocol (GRP), or Optimized Link State Routing (OLSR) protocol can be selected. There are abundance of options left to set different routing protocol parameters. It is also possible to specify WLAN MAC address, channel settings (e.g. transmit power, threshold), Point Coordination Function (PCF), and Distributed Coordination Function (DCF) parameters.

Wireless Local Area Network Workstation (WLANW): this model has similar attributes as WLANS. There is option to select it as mobile node or fixed node. Identical routing protocols as WLANS are available. Overall, analogous architecture is present for both the node models except their functionality and contribution to the network. WLANW could be used to construct different network technologies one of them is Ad-Hoc network. However, modifications were made to the OPNET standard *wlan_wkstn_adv* to create a IEEE 802.11p node model.

2-3 Vehicular channel models

Wireless channels are sensitive to the propagation environments. Signal can be reflected, absorbed, diffracted, or scattered by objects in the environment. In case of channels for V2V communication, abrupt signal level fluctuation may occur due to reflection by roads and vehicles in the range, diffraction by road side buildings and structures, scattering by trees and terrains. This section illustrates channel modeling concepts and present developments in the vehicular use case.

2-3-1 Large scale fading

The term large scale fading is used to describe average power attenuation of a transmitted radio signal. Large scale fading usually combines overall effect of path loss and shadowing which is shown in Fig. 2-6. Due to the property of propagation environments and indulgence of power radiated by transmitter over distance average, signal level drops to a certain number and is defined as path loss. Signal level fluctuation due to path loss occurs over few hundred meters to kilometer. Whereas, the existence of obstructing objects in between transmitter and receiver results in attenuated signal envelop through reflection, scattering, diffraction, and absorption which is called shadowing. It is evident that shadowing appears over distances of 10 meters to 100 meters.

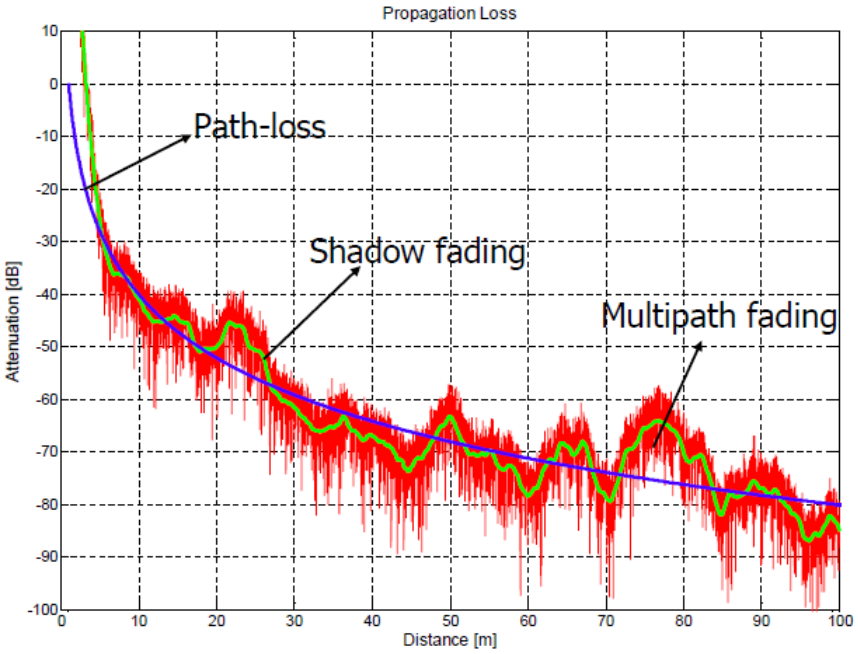

Figure 2-6: Large and small scale propagation effects over distance.

Since amplitude fading respect to path loss and shadowing become visible over larger distances, these effects are called large scale propagation effects.

2-3-1-1 Free space path loss model

The free space propagation model assumes clear, unobstructed Line of Sight (LoS) path between transmitter (Tx) and receiver (Rx) [19]. Separation distance between transmitter and receiver is considered as parameter to measure received power. The Friis equation for calculating free space received power (P_r) is,

$$P_r(d) = P_t G_t G_r \frac{\lambda^2}{(4\pi)^2 d^2 L}. \tag{2-1}$$

Where, P_t is transmitted power, G_t and G_r are Tx and Rx antenna gain respectively, λ is the wavelength of the operating frequency, d is the propagation distance, and L is the system loss not related to propagation. It is customary to represent path loss as a positive quantity measured in dB and defined as difference between effective transmit power and received power. In this thesis work Tx and Rx antennas are considered as omnidirectional. As a result antennas have unity gain. Then the path loss can be derived as,

$$PL(dB) = 10\log_{10}\frac{P_t}{P_r} = -10\log_{10}\left[\frac{\lambda^2}{(4\pi)^2 d^2}\right]. \tag{2-2}$$

2-3-1-2 Two-ray model

The two-ray model is one of the simplest propagation model which considers a direct path and a reflected path from the surface of the earth. Detail about the model and

parameters could be found in any known literature. In [19], the simplified two-ray model was derived as,

$$P_r(d) = P_t G_t G_r \frac{h_t^2 h_r^2}{d^4}, \tag{2-3}$$

where, h_t, and h_r are transmitter and receiver antenna height respectively.

2-3-1-3 Empirical path loss model

Free space propagation model is based on the assumption of no obstacles in between Tx and Rx which does not represent real life propagation scenarios. As a result, more accurate models are needed to encounter complex propagation environment. In the present literature most of the path loss models are based on empirical measurements. However, only Dual Slope Piecewise Linear (DSPL) model possesses specific parameter sets to define different vehicular scenarios i.e. urban, suburban, highway, and rural. This model varies the path loss exponent depending on the propagation distance to address certain large scale fading for specific environment. In [20] and [21], Lin Cheng has defined DSPL path loss exponents along with standard deviation. The model parameters were extracted solely based on measurement campaigns. These path loss exponents and standard deviation values will be used for large scale simulation of V2V communication which is one of the major contributions of this graduation project. The generic form of widely used log normal model is defined as,

$$P(d) = P(d_0) + 10\gamma log10\left(\frac{d}{d_0}\right) + X_\sigma, \tag{2-4}$$

where, γ is the path loss exponent, and X_σ is the zero mean normally distributed random variable with standard deviation σ. This model also describes random shadowing effects which may occur over a large number of locations for same Tx-Rx separation, but different level of obstructions during the propagation. This phenomenon is called log-normal shadowing [19].

DSPL model is a special case of piece wise linear model [20]. Empirical measurements depict dual slope path loss model fits measurements more accurately. Lin Cheng has characterized this piecewise model by a path loss exponent γ_1 and a standard deviation σ_1 within a critical distance d_c. If wave travels more than d_c, power decays with another path loss exponent γ_2 with a standard deviation σ_2. The model can be expressed as,

$$p(d) = \begin{cases} p(d_0) - 10\gamma_1 log_{10}(\frac{d}{d_0}) + X_{\sigma_1} & if\ d_0 \leq d \leq d_c \\ p(d_0) - 10\gamma_1 log_{10}(\frac{d_c}{d_0}) - 10\gamma_2 log_{10}(\frac{d}{d_c}) + X_{\sigma_2} & if\ d > d_c. \end{cases} \tag{2-5}$$

In equation (2-5),

$P(d_0)$ = received signal strength at a reference distance d_0,
γ_1 = path loss exponent till the critical distance d_c,
γ_2 = path loss exponent beyond the critical distance d_c,
X_{σ_1} = zero mean normally distributed random variable within d_c and,
X_{σ_2} = zero mean normally distributed random variable beyond d_c.

Table 2-5: DSPL parameter values for different scenarios

Parameters	Urban	Suburban	Rural	Highway
γ_1	1.656	2	2.3	1.9
γ_2	1.755	4	4	4
d_c	10m	100m	226m	220m
σ_1	Nakagami	5.6	5.8	5.5
σ_2	Nakagami	8.4	6.7	4.9

By considering smooth ellipsoid earth model, d_c is the distance where first Fresnel zone touches the ground and said as Fresnel distance. This distance maintains strict relationship with Tx height (h_t), Rx height (h_r), and wave length at 5.9 GHz frequency. Fresnel distance d_F can be defined as,

$$d_F = \frac{4h_t h_r}{\lambda}. \tag{2-6}$$

However, d_c can be also taken as adjustable parameter for more accurate fitting of measurement data set.

One of the particular objectives of this research is to find out suitable channel models for different vehicular scenarios. Scenarios can be differentiated depending on vehicle speed, traffic density, terrains, buildings, number of road-lanes, separation, vehicle types, and presence of scatterers. After extensive literature survey it was concluded that propagation environment for V2V communication can be divided into the following four scenarios:

- Urban
- Suburban
- Rural and
- Highways.

For all these cases, DSPL model was used for characterizing large scale path loss. For the sake of maintaining fidelity of large scale simulation results, only the model parameters acquired through empirical measurements will be used in this paper. Such parameter values are evident in [20] and [21] for suburban, rural, and highway territories. Where as, in [22] G. P. Grau et al. has used CVIS OBU equipment to measure dual slope path loss exponents for urban scenario with the varying vehicle speed. All these values are assembled in Table. 2-5. However, simulation results retrieved from suburban, rural, and highway scenarios will be discussed in this research as less discrepancy was found in the presented empirical parameters for these scenarios.

2-4 Conclusion

Vehicle to vehicle communication differs from traditional Ad-Hoc network particularly because of it's decentralized architecture and highly dynamic topology. In this

chapter, IEEE proposed IEEE 802.11p standard was outlined to provide basic understanding of the standard. This standard was implemented in OPNET based 802.11p node model. The WAVE PHY layer was illustrated where number of channels, bandwidth allocation, and other physical layer specifications were discussed. Then MAC layer specifications of IEEE 802.11p were reviewed. It was also explained how quality of service can be implemented in WAVE for different types of channels with different classes of traffic using EDCA and IEEE 1609.4. In the last section, vehicular channel models for urban, suburban, highway, and rural scenarios were adumbrated. In the subsequent chapters, the developed IEEE 802.11p node model used in the simulation scenarios and more realistic channel models for V2V communication will be presented.

Chapter 3

OPNET simulation platform and the node model

3-1 Introduction

OPNET Modeler is one of the most advanced network simulators for designing and analyzing different communication networks, devices, protocols, and applications [27]. The modeler has the fastest Discrete Event Simulation (DES) engine among the leading industry solutions along with hierarchical modeling environment and object-oriented modeling. In this research, OPNET Modeler 14.5 was used to develop the node model. However, literature survey showed that there is no network simulators at this time that own standardized IEEE 802.11p node model. OPNET is not an exception. Furthermore, like most of the network simulators OPNET does not consider realistic radio propagation channel models for wireless communications which may lead to erroneous and overly optimistic results for implementing in actual systems. In this chapter, details about the elements required for setting up vehicular scenarios in OPNET platform and the novel 802.11p node will be discussed along with parameters of the standard.

3-2 Elements of an OPNET vehicular scenario

The 802.11p node model was developed based on previously discussed *wlan_wkstn_adv*. However, the node model was evolved before the standardization of Dedicated Short Range Communications (DSRC) by IEEE. As a consequence, necessary modifications were made to the node model to meet the standard. In Fig. 3-1, a simple vehicular scenario is presented with 29 802.11p mobile nodes. In the figure, we can see vehicle nodes are distributed over four different trajectories. Nevertheless, in the simulation study for retrieving results using different vehicle to vehicle wireless channel models more realistic scenarios will be presented in the simulation chapter. In the figure below, the unit of span of the network was selected as meters, initial topology was chosen to be a empty scenario, and scale of the network was taken as office network. This figure gives an impression how the scale, topology, and network technology can be implemented at

the top of the OPNET modeling hierarchy. Four different trajectories are also visible in the project editor. Trajectories can be used to define roads and number of lanes through which vehicles will change its position during simulation. The arrow sign at the end of the each trajectory depicts the direction towards which vehicles will move. Though trajectories allow us to define certain paths for the mobile nodes, OPNET does not have road or infrastructure models for more realistic environment to be used in vehicular networks.

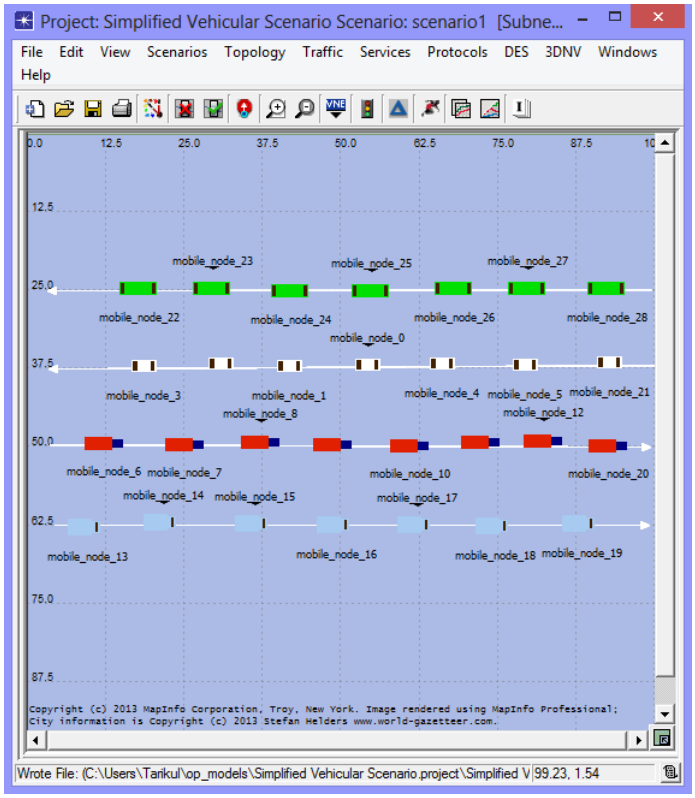

Figure 3-1: Simplified vehicular scenario with defined trajectories.

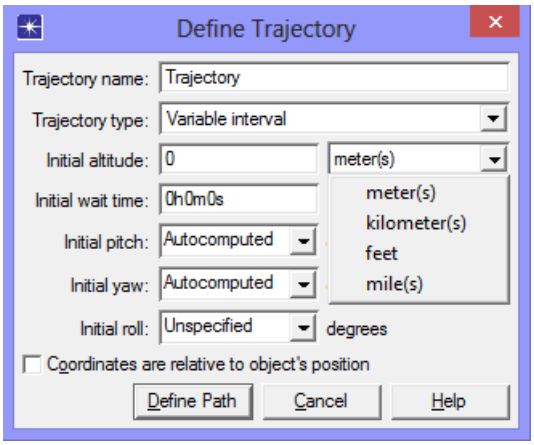

Figure 3-2: OPNET trajectory editor.

3-2-1 Trajectory definition

The trajectory editor is a very important tool for defining mobility of different types of nodes. The application ranges from satellite orbit to aircrafts but not limited to vehicular use case for both the civil and defense applications. Each of the nodes can be assigned a specific trajectory as a function of time. In case of wireless mobile nodes it is required to have persistent models of mobility that can represent time varying nature of separation distance between transmitter and receiver. Fig. 3-2 outlines different trajectory parameters. In the trajectory type drop down menu variable interval or fixed interval can be chosen. Variable interval trajectory facilitates setting up initial altitude and initial wait time. For the specified initial wait time period the node will stay in that point before moving to the next trajectory segment. On the other hand, a fixed interval trajectory specifies the amount of time it will take to pass the segment. Other entries for trajectory definition shown in the figure can be used to set initial conditions.

One of the major characteristics of vehicle to vehicle communication is moving transmitters (Tx) and receivers(Rx) which may play a key role to reduce connectivity and quality of communication. Increasing velocity of Tx and Rx will generate Doppler shift which will modulate center frequency of the signal in a random manner. As a result, higher signal level fluctuation will be observed by the receivers. Hence, heavily fluctuating Signal to Noise Ratio (SNR) and higher Bit Error Rate (BER) will be attained. Details about the communication channels will be discussed in the next chapter. From the discussion about Fig. 3-2 we have seen defining series of discrete positions, speed, and bearing how the mobility of the vehicles can be implemented in OPNET.

To represent more realistic presentation of different scenarios (e.g. suburban, highway) velocity of the vehicles were chosen from real life traffic velocity in the corresponding scenario. As an example, in suburban scenario average velocity of the traffic is 20 km/hr to 45 km/hr which is less than highway scenario due to more frequent road signals and speed limit in the area. Different units (e.g. meters, kilometers, feet, miles) can be used in the trajectory editor to scale down the paths with scenario span. This is particularly useful for communication range. The intended communication range for

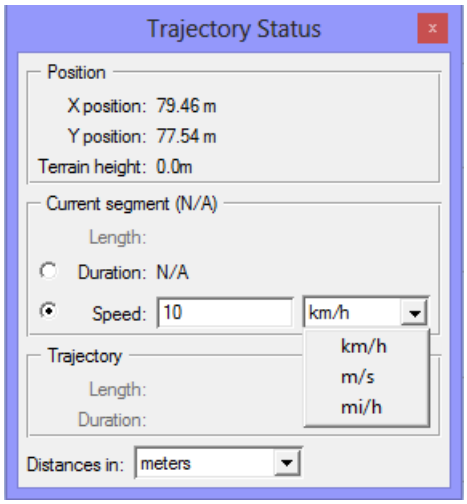

Figure 3-3: Trajectory status editor for defining variable speed.

Intelligent Transportation Systems (ITS) applications is 1000 meters, as a result in this study all the trajectory distance, speed, and altitude vales were taken in meters. There is option available to set up coordinates of a trajectory relative to object's position. If a single trajectory is assigned to all the active nodes in the network, this will facilitate varying relative speed without assigning specific velocity for each of the node. For a very large network it could be a useful option. In Fig. 3-3, we can see the status editor which pops up while setting up trajectory in the project editor. The mentioned editor can be used to set up different vehicle speed with transverse trajectory segments. X and Y coordinates are also visible in the figure which continuously change with defining cursor position and enable more accurate trajectory assignment.

3-2-2 OPNET mobility model

In OPNET it's also possible to define mobility of the nodes by using *mobility config* object model. Mobility of a network can be defined by a mobility domain and a mobility profile. A user has the freedom to create his/her own mobility profile or to use default mobility models. One mobility object can hold multiple mobility profiles. However, a scenario with random mobility must use unit of degrees. In the Fig. 3-4, attributes of the mobility object model is presented. In the figure we can see three different random mobility profiles, where user defined mobility domain can be selected. The algorithm used to characterize movements of the nodes are Random Waypoint Model (RWM). The RWM is based on the concept that destination, speed, and direction are all randomly chosen independent of other nodes. The *x_min, y_min, x_max*, and *y_max* values could be used to bound the nodes so that they can maneuver only within the specified region. This mobility model is particularly useful for Ad-Hoc network. Nevertheless, for vehicle to vehicle communication major concern should be defining roads and lanes with specific direction of the moving vehicles. Unfortunately, RWM is unusable to model such scenario due to it's random nature. As a result, in this study trajectory was chosen to implement mobility instead of using random way point model.

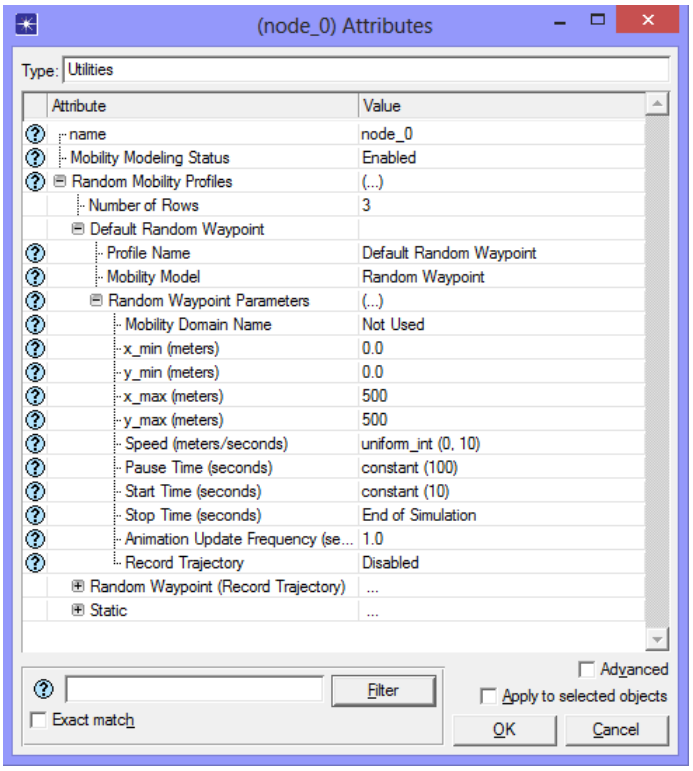

Figure 3-4: Mobility configuration node attributes.

3-2-3 The IEEE 802.11p node model

In this section detail about IEEE 802.11p node model will be presented. The basic model was originally developed by University of Surrey [37]. It was developed further by Netherlands Organization for Applied Scientific Research (TNO) by including IP Type of Service (ToS) to Wireless Local Area Network (WLAN) Quality of Service (QoS) mapping, and modified traffic generator. During this MSc thesis required amendment was made to the node model to meet the standard. Concepts and proposed standard Physical Layer (PHY) and Medium Access Control (MAC) layer parameters were discussed in the previous chapter. In Fig. 3-5, the hierarchical architecture of the node is presented. However, discussion about the node will be limited to PHY and MAC layer. In the figure we can see the following four modules of the node that perform functionality of PHY and MAC layer,

Antenna
: This module is used to exchange packets with other mobile nodes. The antenna gain and directivity can also be modeled using antenna pattern editor.

wlan_port_rx
: Receiver module performs the task of receiving packets via radio links.

wlan_port_tx
: The transmitter module collects packets from one or more input packet streams and transmits them over the corresponding communication channel.

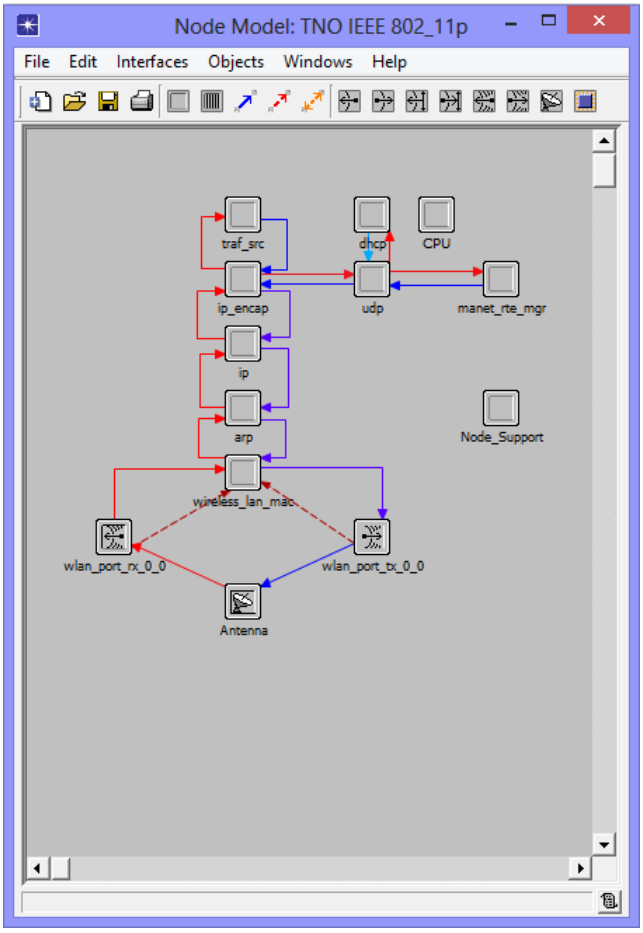

Figure 3-5: TNO's IEEE 802.11p node model.

wireless_lan_mac
: This module enables MAC layer functionality of the model which is independent of higher layer modules.

The discussed modules will be elaborated in the following subsections.

3-2-3-1 Physical layer attributes

In the previous section functionality of PHY and MAC layer modules were briefly outlined. In this section of the chapter physical layer parameters will be illustrated along with the relevance in relation to IEEE 802.11p standard.

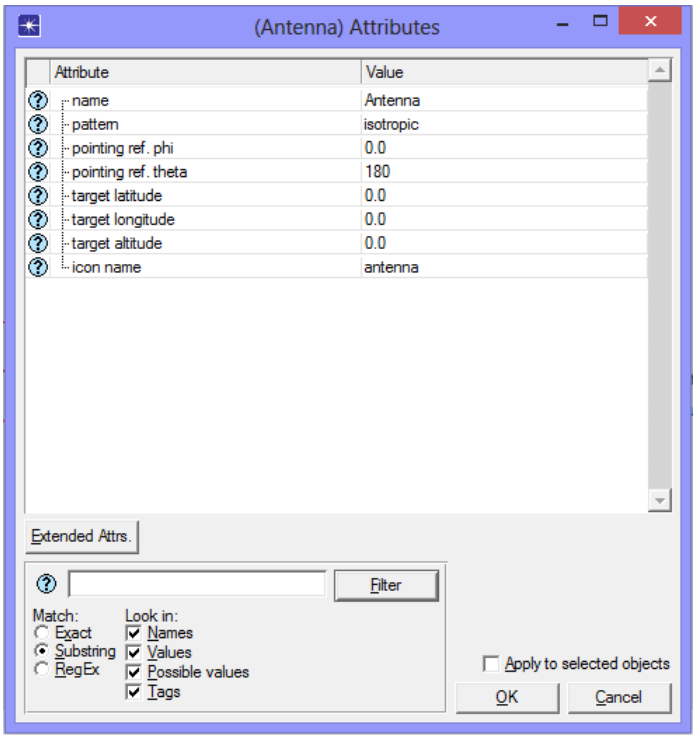

Figure 3-6: Attributes of the antenna.

3-2-3-1-1 Antenna module

Antenna module consists of six attributes which defines gain, radiation pattern, directivity, and reference points towards which antenna will pointed. In Fig. 3-6, a snap shot of the antenna module attributes are presented where we can see isotropic antenna was chosen. In recent years much effort has been put to analyze effects of directional antennas which may yield substantial performance improvements of IEEE 802.11p networks [28]. Though use of directional antenna may enable more persistent communication, in heavy traffic situation such use may result in higher number of nodes to be deprived of communication due to blockage of radio waves by other vehicles in between. Directional antennas could be particularly useful for fixed Road Side Unit (RSU) when pointing towards specific direction will contribute for higher number of vehicles in the range and higher numbers of successful transaction of messages. Since, the major research goal of this thesis is to analyze vehicular channel models using IEEE 802.11p nodes, for simplification omnidirectional antenna was selected. Isotropic antennas radiate power equally in all directions as a result it has gain of 0 dB at all points.

3-2-3-1-2 Transmitter module attributes

The transmitter module plays a key role in collaboration with the antenna to establish links with radio receivers. Generated input packet streams are collected by this module and transmitted over the channel with the same index number. Channel settings, modulation, and different pipeline stages are presented in the Fig. 3-7. In

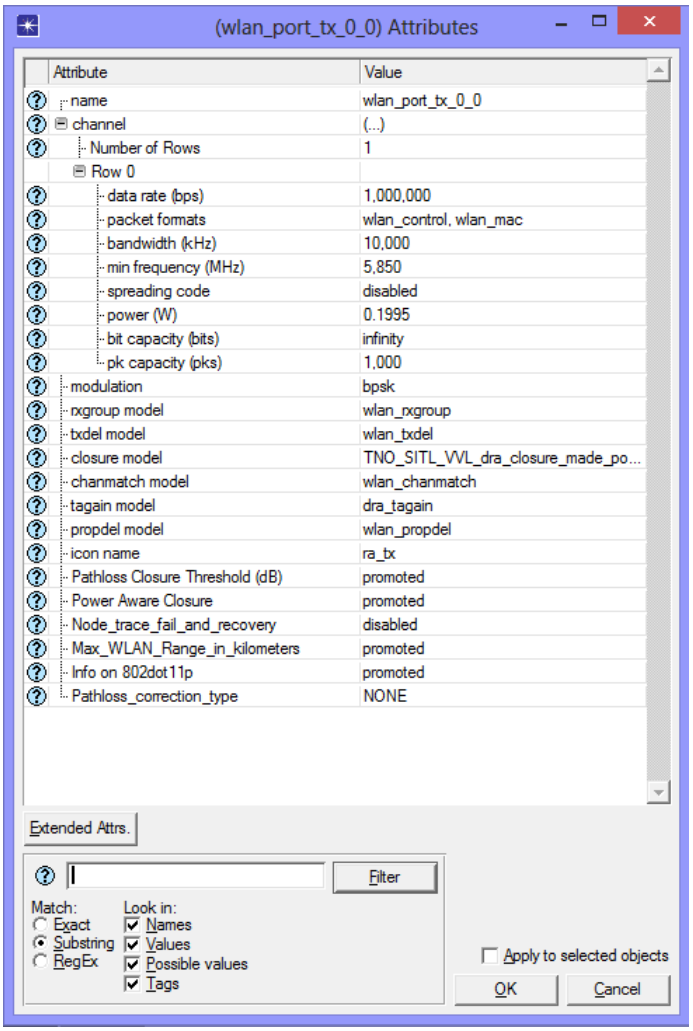

Figure 3-7: Transmitter module attributes.

the figure we can see the transmitter uses six pipeline stages. Detail about pipeline stages will be discussed in the simulation chapter. To meet the 802.11p PHY standard frequency, bandwidth, and transmit power was set to 5850 MHz, 10 MHz, and 0.1995 Watt (23 dBm) respectively. From the list of modulation tables Binary Phase Shift Keying (BPSK) was selected. This modulation technique is the most robust among all Phase Shift Keying as highest level of noise or distortion is required to be misinterpreted by a demodulator. For higher data rate the DSRC standard supports Quadrature Phase Shift Keying (QPSK), 16 Quadrature Amplitude Modulation (QAM), or 64 QAM. The *rxgroup* model determines possibility of connection between each radio transmitter channel and each receiver channel in the network. The IEEE 802.11p standard specifies maximum allowable communication range as 1000 meters. To implement this range in the simulation scenarios *Max_WLAN_Range_in_Kilometers* model was programmed in such a way that receivers distant beyond 1 km from the transmitting node are excluded to be considered as potential candidates for receiving the messages. As a result, excluding these distant nodes before start sending messages will reduce unnecessary

generation of packets and higher simulation efficiency can be achieved. *Pathloss Closure Threshold* is another way of deciding whether communication is possible or not. During execution pathloss will be calculated depending on range and other antenna parameters. Be the pathloss value is below threshold the receiver will be left out as a destination. The *rxgroup* model determines possibility of connection between each radio transmitter channel and each receiver channel in the network. Couple of examples for clarification can be transmitter should not hear it's own transmission and receivers only within the current subnet should be potential destination. The IEEE 802.11p standard specifies maximum allowable communication range as 1000 meters. To implement this range in the simulation scenarios *Max_WLAN_Range_in_Kilometers* model was programmed in such a way that receivers distant beyond 1 km from the transmitting node are excluded to be considered as potential candidates for receiving the messages. As a result, excluding these distant nodes before start sending messages will reduce unnecessary generation of packets and higher simulation efficiency can be achieved. *Pathloss Closure Threshold* is another way of deciding whether communication is possible or not. During execution path loss will be calculated depending on range and other antenna parameters. If the path loss value is below threshold the receiver will be left out as a destination.

3-2-3-1-3 Receiver module attributes

The receiver module has similar attributes as the transmitter module. It is very important to match Tx-Rx physical parameters (e.g. carrier frequency, bandwidth, modulation) otherwise all the data packets will be dropped during execution of channel match pipeline stage. As a consequence, in Fig. 3-8 we can see receiver channel settings were set to exactly same as Tx channel settings. The receiver Noise Figure (NF) was used to represent effect of receiver's thermal noise on transmission. It is customary to calculate NF based on bandwidth and standard temperature. NF was set to 3 dB by considering minimum detectable signal strength for 10 MHz bandwidth. The *ecc threshold* specifies maximum number of allowable bit errors in a packet which was set to zero. That means packets with any number of error bits will be dropped by the receiver. Like the Tx module, the Rx module invokes several pipeline stages. Few of them are to mention *ragain*, *power model*, *bknoise*, *inoise*, *snr*, *ber*, *error model*, and *ecc model*. All these pipeline stages will be explained in the simulation chapter. *Overall additional pathloss attribute* defines an additional path loss at the receiver side. It can be used, for instance to model the total cable losses (sum of loss at the transmitter and the receiver side) or to tune the sensitivity of the radios to measured values.

3-2-3-2 Medium Access Control (MAC) layer attributes

The MAC module in the node model enables to set MAC layer parameters and their values. We can see in Fig. 3-9 different MAC layer entities along with transmit power, and packet reception threshold. In OPNET it's also possible to get access to these values directly from project editor. For the sake of compatibility the channel settings were kept same as Tx or Rx channel settings which were discussed in the previous

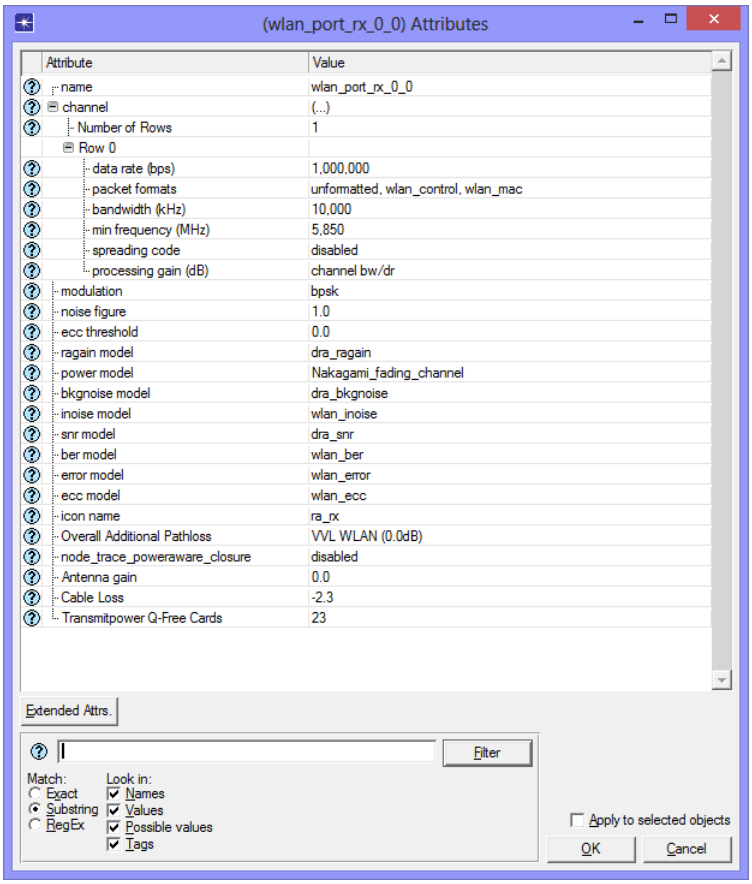

Figure 3-8: Receiver module attributes.

sub-sections. The transmit power was set to 23 dBm which was defined in IEEE PHY layer specification. The *Packet Receiption-Power Threshold* was set to -89 dBm. However, in the literature -95 dBm or some cases -110 dBm were used as threshold. The arriving packets with power less than the threshold are not decoded by the receiver and considered as noise. Packets containing power higher than the threshold are sensed by the MAC layer and can be accepted if the number of error bits remain under bit error tolerance. Few major reasons for bit errors will be discussed in the future chapters. The *Physical Characteristics* was set to Orthogonal Frequency Division Multiplexing (OFDM) to meet IEEE 802.11p standard specification. The WLAN MAC uses this technology to configure Short Inter Frame Spacing (SIFS), slot time, minimum contention window size, maximum contention window size, and DCF Interframe Space (DIFS). Where as, *Data Rate* determines the rate (6 Mbps) at which MAC will transmit data frames over the physical layer. The data rate also depends on used PHY layer technology. Please note that in our simulation study only the service channel was used to reduce complexity of simulating node. Since, Wireless Access in Vehicular Environments (WAVE) supports QoS, Distributed Coordination Function (DCF) was enabled with different classes of traffic and Point Coordination Function (PCF) was kept disabled. For priority specification default Enhanced Distributed Channel Access (EDCA) parameters were tabulated in Table. 2-4. In the Fig. 3-10, it is noticeable that all those

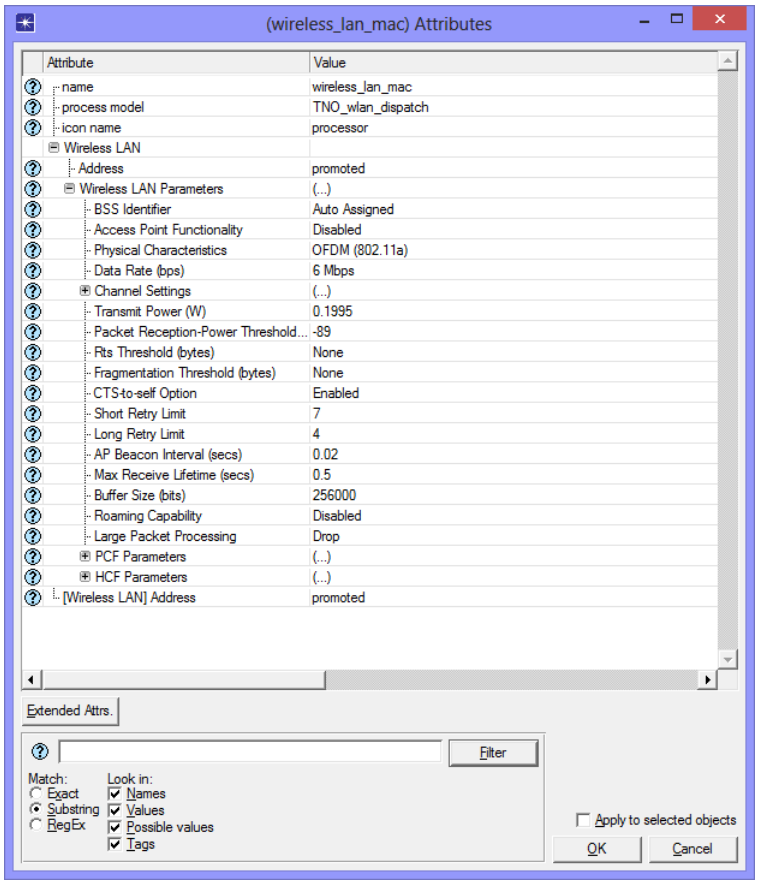

Figure 3-9: MAC layer attributes.

values were set to the developed IEEE 802.11p node model.

3-3 Conclusion

OPNET Modeler is a high fidelity simulation platform which posses wide variety of built in components for designing, simulating, and analyzing almost all kinds of wireless networks. At the beginning of this chapter hierarchical modeling in OPNET was presented. Then wireless model suite was briefly outlined. To obtain feasible results from the study of vehicle to vehicle communication it is mandatory to consider varying vehicle velocity. Hence, in Section 2 of this chapter it was described how trajectory and OPNET mobility model can be used to define paths for mobile nodes. In the following sections, IEEE 802.11p node model was covered along with it's different PHY and MAC layer attributes and parameters. In the node model section four different modules that enable the 802.11p functionality were presented. Then their attributes were elaborated in the following subsections. It was also shown that all the values were chosen so that the node model converges the standard.

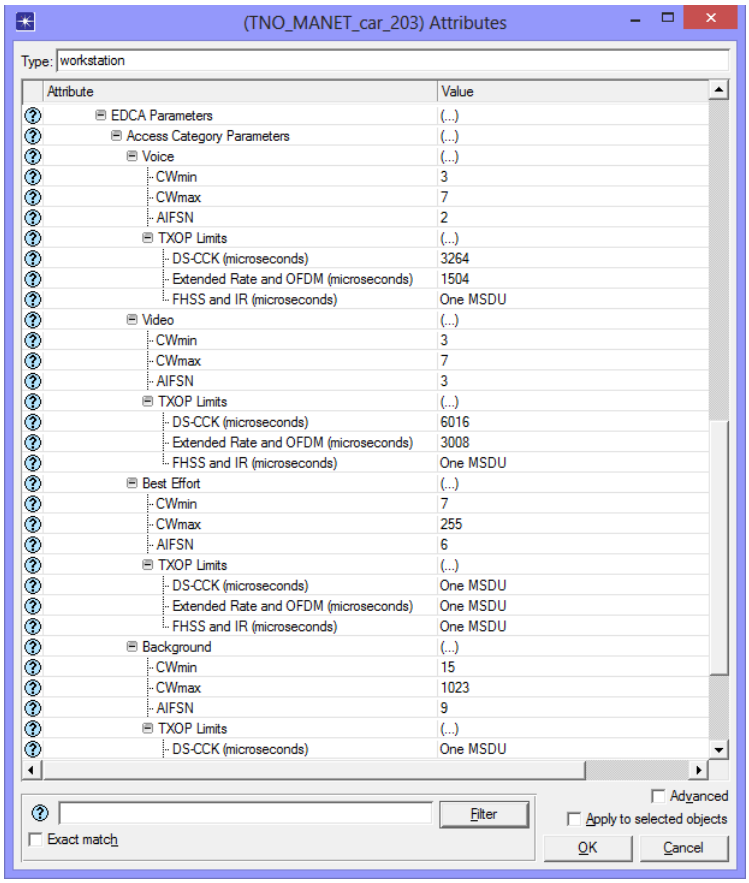

Figure 3-10: EDCA Parameters for different AC.

Chapter 4

Statistical description of vehicular channel models

4-1 Introduction

By the fact that vehicular communication environments change over time and behavior of vehicles are time varying, it becomes more difficult to determine fading of signals. Moreover, due to ground irregularities and low antenna elevations the direct path between transmitter and receiver can be obstructed. In view of the possible presence of variety of environment universal deterministic modeling of vehicular channels is impossible [17]. As a result proven statistical channel models are required to represent real life scenarios. In this chapter, small scale propagation effects due to multipath components will be discussed in details. Furthermore, a novel technique to comprise signal fading for varying propagation environment with transmitter and receiver separation distance will be presented.

4-2 Multipath propagation channel model

Small scale fading is one of the many impairments inherently present in the wireless communication due to presence of scatters and reflectors on the way of radio wave propagation. Mentioned factors effectively contribute to bring forth multiple replicas of the same signal at the receiver. Each of the impersonated version of the original signal comes towards the receiver with distorted amplitude, phase, and angle of arrival. Multipath propagation results in heavily fluctuating signal amplitude. Moreover, for vehicle to vehicle communication when both Tx and Rx are in motion, this motion induces Doppler shift to the received signal frequency and randomly modulates the operating carrier frequency. Multipath propagation delays can contribute to time dispersion of the received signal. In this Section of the report, signal theory and statistical channel models to address small scale fading will be discussed.

4-2-1 Fading statistics for Vehicle to Vehicle (V2V) communication

Multipath channels are defined statistically as it is almost impossible to provide a generic deterministic channel model. As a result, it is customary to present multipath propagation of a radio channel by time varying impulse response of the channel [18]. In this section, statistical characterization of the multipath propagation channel will be presented. The transmitted signal model can be written as,

$$s(t) = \mathfrak{Re}(u(t)e^{j2\pi f_c t}) = \mathfrak{Re}\left\{u(t)\cos(2\pi f_c t)\right\} - \mathfrak{Im}\left\{u(t)\sin(2\pi f_c t)\right\}, \tag{4-1}$$

where, f_c is the carrier frequency, and $u(t)$ is the complex envelope of $s(t)$. Then the received signal can be expressed in terms of sum of all resolvable multipath components and Line of Sight (LoS) component which is,

$$r(t) = \mathfrak{Re}\left\{\sum_{n=0}^{N(t)} \alpha_n(t)u(t-\tau_n(t))e^{j(2\pi f_c(t-\tau_n(t))+\phi_{Dn})}\right\}. \tag{4-2}$$

In the above equation,

$N(t)$ is the number of resolvable multipath components,
α_n is the amplitude of n^{th} multipath component,
τ_n is the corresponding delay, and
ϕ_{Dn} is the Doppler shift due to Tx Rx motion.

It should be noted that for $n = 0$, (4-2) represents only the LoS component of the signal. The occurrence of multipath components may become visible due to presence of several reflectors or scatterers. If each of the mutipath components corresponds to a single reflector the associated phase shift and Doppler shift are $e^{-j2\pi f_c \tau_n(t)}$ and $f_{Dn}(t) = v\cos\theta_n(t)/\lambda$ respectively (v is the velocity of the mobile node, θ_n is the angle of arrival, λ is the wavelength of the transmitted signal). Delay difference of subsequent multipath components and bandwidth of the signal are very important parameters to separate multiple replica of the signal. For example, if two multipath components arrive at receiver with delay τ_1 and τ_2, and their delay difference $\tau_1 - \tau_2$ does not exceed inverse of the signal bandwidth (B_u) then the two components can not be resolved. Channel with this particular characteristic is called the narrowband channel. In contrary, if the delay difference $|\tau_1 - \tau_2| >> B_u^{-1}$, then the multipath components can be differentiated from each other which is called wideband channel. For the former case several version of the signal will be added by the receiver. Hence, constructive and destructive addition of non-resolvable multipath components will result in heavy fluctuation of signal strength. This is called small scale fading. For vehicle to vehicle communication small scale fading may result in heavily fluctuating Signal to Noise Ratio (SNR) and Bit Error Rate (BER). As a consequence, small scale fading has been extensively studied in literature to mitigate, and to predict channel conditions. For simplification of (4-2), $\phi_n(t)$ can be written as,

$$\phi_n(t) = 2\pi f_c \tau_n(t) - \phi_{Dn}. \tag{4-3}$$

Then (4-2) reduces to,

$$r(t) = \mathfrak{Re}\left\{\left[\sum_{n=0}^{N(t)} \alpha_n(t)e^{-j\phi_n(t)}u\left(t-\tau_n(t)\right)\right]e^{j2\pi f_c t}\right\}. \tag{4-4}$$

In (4-4), we can see the amplitude of the signal $\alpha_n(t)$ is a function of path loss and shadowing. Where, phase term $\phi_n(t)$ comes from Doppler, and delay. The Doppler and delay can be modeled as two independent random processes. Delay spread is a way of characterizing wireless channels which is typically measured relative to the received signal component to which demodulator is synchronized. The synchronization can be done with reference to LoS. Normally LoS has the smallest delay τ_0 and maximum delay spread can be derived as, $T_m = max_n(\tau_n - \tau_0)$. Moreover, mean delay $\bar{\tau_0}$ of collective multipath components can also be used as reference for measuring delay spread. In that case, the delay spread can be obtained as, $T_m = max_n(\tau_n - \bar{\tau_0})$. However, the variable T_m may become random in nature for time varying channel and random number of multipath components may arrive at the receiver with very weak signal strength. As a result, it is customary in wireless communication to portray delay spread relative to power delay profile which mitigates the limitations of delay spread mentioned above. The power delay profile enables to determine meaningful channel statistics like average delay spread and rms delay spread. Nevertheless, these higher order statistics will not be discussed in this report as main goal of this thesis is to analyze IEEE 802.11p using appropriate vehicle to vehicle channel models. As a result, discussion will be limited to large and small scale fading with their effects on Signal to Interference and Noise Ratio (SINR) and BER.

4-2-2 Narrowband channel model

As already discussed in the previous section when delay spread of the channel is small relative to the inverse of the signal bandwidth then the channel becomes a narrowband channel. This is a realistic assumption for vehicle to vehicle communication [29] due to the fact that allowable communication range is very short, most of the times clear LoS component will be visible to the receiver, and reflection due to nearby objects will generate multipath components. Consequently, delay spread of the channel will be small compared to inverse of the signal bandwidth. Most of the channels for wireless communications hold narrowband assumption. Hence, the frequency response of the channel can be considered as flat fading which simplifies analysis of the channel greatly. Moreover, narrowband stochastic channel models focus on the characteristics of the Doppler spectrum, which is a key quantity that distinguishes a V2V channel from a cellular channel [30]. Under the described narrowband assumption, delay associated with i^{th} multipath component is $\tau_i \leq T_m \forall i$, which implies that $u(t-\tau_i) \approx u(t) \forall i$. In that case, (4-4) reduces to,

$$r(t) = \mathfrak{Re}\left\{u(t)e^{j2\pi f_c t}\left(\sum_n \alpha_n(t)e^{-j\phi_n t}\right)\right\}. \tag{4-5}$$

If we choose an unmodulated carrier $s(t) = cos(2\pi f_c t - \phi_0)$ with random phase offset ϕ_0 and a single pulse $u(t) = 1$ the equation for received signal further reduces to,

$$r(t) = \mathfrak{Re}\left\{\left[\sum_{n=0}^{N(t)} \alpha_n(t) e^{-j\phi_n t}\right] e^{j2\pi f_c t}\right\} = r_I(t)\cos(2\pi f_c t) + r_Q(t)\sin(2\pi f_c t), \quad (4\text{-}6)$$

where, in phase and quadrature phase components can be defined as,

$$r_I(t) = \sum_{n=1}^{N(t)} \alpha_n(t)\cos(\phi_n(t)), r_Q(t) = \sum_{n=1}^{N(t)} \alpha_n(t)\sin(\phi_n(t)). \quad (4\text{-}7)$$

From the narrowband fading model presented above it is noticeable that both the delay and Doppler are incorporated in the model. For large number of multipath components, according to Central Limit Theorem the inphase and quadrature phase components are Gaussian processes given that $\alpha_n(t)$ and $\phi_n(t)$ are stationary and ergodic processes. Stationary process is the process whose probability distribution does not change when shifted in time of space. Whereas, a stochastic process is said to be ergodic if its statistical properties can be derived from a single, sufficiently long sample. For small number of N if the amplitude terms are Rayleigh distributed and phase terms are Uniformly distributed on $[-\pi, \pi]$, then the inphase and quadrature phase terms still posses the Gaussian property. This property greatly simplifies further analysis of the fading envelope of the signal due to multipath propagation.

4-2-3 Correlation and spectral properties of vehicle to vehicle channel

To characterize fading channels and evaluate performance of communication, it is necessary to distinguish between slow and fast fading which are another two impairments for wireless communications. As a result, coherence time T_c of the channel which is the period of time over which the fading process is correlated must be addressed in the fading analysis. The most important property of vehicle to vehicle channel Doppler spread f_d is directly related to coherence time of the channel which can be defined as [31],

$$T_c \simeq \frac{1}{f_d}. \quad (4\text{-}8)$$

If the coherence time of the channel is greater than symbol duration T_s then the channel is said to be slow fading channel. On the other hand, when coherence time is less than T_s the channel is a fast fading channel. In slow fading channel fading may affect many consecutive symbols which results in burst errors. On the other hand, fast fading channel imposes heavily fluctuating amplitude and phase. As a result autocorrelation function is used to assess the effect of fluctuation. For cellular networks in [18] autocorrelation function was derived as,

$$\begin{aligned} \mathcal{R}_{r_I}(\tau) = \mathcal{R}_{r_Q}(\tau) &= \frac{P_r}{2\pi}\int \cos(2\pi v t\cos\theta/\lambda)d\theta \\ &= P_r J_0(2\pi f_d \tau), \end{aligned} \quad (4\text{-}9)$$

where,

$$J_0(x) = \frac{1}{\pi}\int_0^{\pi} e^{-jx\cos\theta}d\theta \tag{4-10}$$

is the zeroth order Bessel function of first kind. For the derivation of (4-9), Wide Sense Stationary Uniform Scattering (WSSUS) environment was assumed. A channel is said to be Wide Sense Stationary (WSS) if it's mean is constant over the period of time of interest and autocorrelation depends only on difference between two time points. This assumption simplifies the derivation of autocorrelation function in a considerable manner. Autocorrelation attains its maximum value at $\tau = 0$. Whereas, if N number of multipath components arrive at the receiver with angle of arrival $\theta_n = n\Delta\theta$ (here $\Delta\theta = 2\pi/N$) then the environment is called uniform scattering environment. This means multiple replicas of the signal arrive at the receiver with uniformly distributed phase between zero and 2π. It was also assumed that, each of the components has the same received power of P_r which implies, $E[\alpha_n^2] = 2P_r/N$.

However, the autocorrelation function discussed above represents traditional cellular network when a fixed base station is present to serve several mobile nodes. But for V2V communication when both the transmitter and receiver are in motion the fluctuation of signal envelope will increase greatly. As a result, appropriate autocorrelation model is necessary to characterize V2V channel model. In [32], [30], and [33] the normalized time autocorrelation function of received complex envelope of two moving vehicles was defined as,

$$\begin{aligned}\mathcal{R}_{r_I}(\tau) = \mathcal{R}_{r_Q}(\tau) &= P_r J_0(2\pi f_1\tau)J_0(2\pi f_2\tau),\\ &= P_r J_0(2\pi f_1\tau)J_0(2\pi a f_1\tau).\end{aligned} \tag{4-11}$$

In the above equation $a = f_2/f_1 = v_2/v_1$, where v_1 and v_2 are Tx or Rx velocity, f_1 and f_2 are the maximum Doppler frequency shift due to transmitter (Tx) or receiver (Rx) motion. If Tx velocity is greater than Rx velocity then Tx velocity should be used as denominator of ratio a. On the other hand, if Rx velocity is greater than Tx velocity then Rx velocity should be used as denominator of ratio a. This is to keep the value of a within the limit of $0 \leq a \leq 1$. Since, fading power spectrum is calculated by taking Fast Fourier Transform (FFT) of the autocorrelation function, this limit is applied to maintain the power spectrum so that the fading envelope would not blow up. It should be noted that for uniformly distributed random phase between $[0, 2\pi]$, Doppler frequency experienced by each path is the sum of the motion induced by motion of Tx and Rx individually. It is also noticeable in (4-11) that, the autocorrelation function is a product of two Bessel functions instead of one Bessel function in conventional cellular communication. Equation (4-11) was used in the simulator which will be described in the next chapter.

Since, the power spectrum of the fading envelope is calculated from autocorrelation function, change in this correlation function has direct impact on signal level fluctuation of received signal. In Fig. 4-1 given below, autocorrelation is presented for three different Tx-Rx velocity pairs. When they are moving with the same speed (a = 1), there is no velocity difference and separation distance does not change in between the

two mobile nodes. As a result, autocorrelation attains lower time lags in between cycles compared to others. It is also noticeable from the figure that for higher speed difference between Tx-Rx pair, the autocorrelation becomes zero for higher values of $f_1\tau$. An interesting interpretation can be made from there is, signal decorrelation time will increase with difference between Tx-Rx velocity pair, that may effectively contribute for more sparse channel for longer period of time. After decorrelation time a heavily fluctuating channel may turn into a reasonably flat channel. However, signal may recorrelates after it becomes uncorrelated. Power spectrum of the received signal can be computed by taking Fourier transform of autocorrelation function. In [33], the power spectrum was presented as,

$$S(f) = \frac{1}{\pi^2 f_1 \sqrt{a}} K \left[\frac{1+a}{2\sqrt{a}} \sqrt{1 - \frac{f^2}{(1+a)^2 f_1^2}} \right], \tag{4-12}$$

where $K[*]$ is the complete elliptic integral of the first kind, and f is a frequency relative to the carrier frequency.

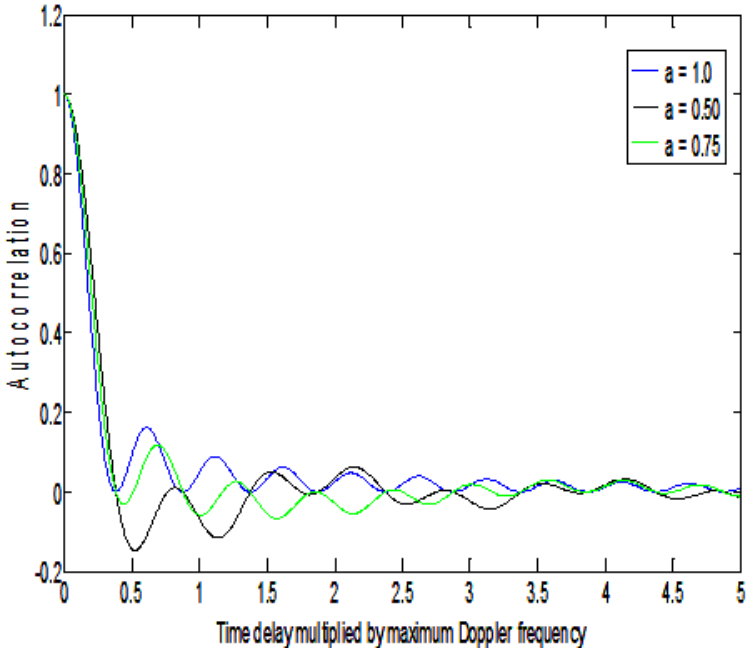

Figure 4-1: Autocorrelation for different values of a.

4-2-4 Statistical modeling of envelope and power distribution

Signal statistics is a way of developing mathematical understanding of the propagation channel as derivation of a ray tracing model requires detail knowledge about the geometry of the propagation environment. For vehicle to vehicle communication when propagation environment is changing with vehicle mobility, it is almost impossible to derive such a model for the mentioned use case. Moreover, data collection scheme from

in-situ test beds for large number of vehicles is always expensive and time consuming. As a matter of fact, suitable stochastic channel model for V2V communication was developed in this research which will be tested for large number of vehicles in the simulation scenarios. Different probability distributions that are used to address multipath fading will be outlined in this section.

If all the multipath components arrive at the receiver with identical signal amplitude then a Rayleigh distribution occurs for the signal envelope. We saw in the previous section, if the phase $\phi_n(t)$ is uniformly distributed then both the inphase and quadrature phase components of the signal envelope are zero-mean Gaussian distributed. From where it can be deduced that the signal envelope is Rayleigh distributed. Based on Central Limit Theorem, the distribution function results from superposition of an infinite number of random variables is a Gaussian function. Signal envelope in relation to inphase and quadrature phase components can be written as,

$$z(t) = |r(t)| = \sqrt{r_I^2(t) + r_Q^2(t)}, \tag{4-13}$$

where, both $r_I(t)$ and $r_Q(t)$ has variance of σ^2. The Rayleigh distributed signal envelope can be written as,

$$P_Z(z) = \frac{2z}{P_r} e^{\frac{-z^2}{P_r}} = \frac{z}{\sigma^2} e^{\frac{-z^2}{2\sigma^2}}. \tag{4-14}$$

In the above equation, $P_r = \sum_n E[\alpha_n^2] = 2\sigma^2$ is the average received power considering path loss and shadowing only.

For vehicle to vehicle communication it is evident that most of the time signal strength will be dominated by strong LoS component. As a consequence, assumption for Rayleigh distribution, multipath components arrive at the receiver with same amplitude does not hold anymore. Then inphase and quadrature phase components have non zero mean and fading envelope should be characterized as superposition of a LoS component and a complex Gaussian component. In this case, the signal envelope is Rician distributed rather than Rayleigh. The probability density function of Rician fading envelope can be written as,

$$P_Z(z) = \frac{z}{\sigma^2} e^{\left[\frac{-(z^2+s^2)}{2\sigma^2}\right]} I_0\left(\frac{zs}{\sigma^2}\right), \tag{4-15}$$

where, s^2 is the power in LoS component.

4-2-4-1 Nakagami-*m* fading channel

In this thesis assignment major focus was given to Nakagami-m distribution which can model signal fading condition that ranges from severe to moderate, to light fading or no fading [34]. Empirical measurements reveal that this distribution fits better for vehicle to vehicle communication. The propagation anomaly discussed earlier can be stochastically modeled using Rician or Rayleigh fading. Nevertheless, Nakagami fading was used in this study because this is a more generalized form of modeling small scale fading and can be transformed into Rayleigh or Rician fading assigning appropriate parameter values in the distribution. Nakagami has presented in [35] that

signal amplitude fading can be expressed as Probability Probability Density Function (PDF),

$$f_Z(z) = \frac{2m^m z^{2m-1}}{\Gamma(m)\Omega^m} e^{-(m/\Omega)z^2}, \tag{4-16}$$

where, signal amplitude $z \geq 0$, $\Omega = E[z^2] = \bar{z^2}$ is the average fading power, $E[\cdot]$ is the expectation operator, and $\Gamma[\cdot]$ is the Gamma function. The fading parameter m which determines severity of fading can be expressed as,

$$m = \frac{(\bar{z^2})^2}{(z^2 - \bar{z^2})^2} \geq \frac{1}{2}. \tag{4-17}$$

In most of the literature Nakagami fading model was implemented for fixed fading parameter-m and constant average velocity. Since, V2V propagation environment changes with vehicle mobility, all the channels will not necessarily suffer same fading. As a result Nakagami-m parameter should vary with varying propagation environment of V2V communication. During this research assignment, a relation between parameter-m and propagation distance was derived using the data set presented in [20]. It was observed while applying linear regression that data set 1 fits better compared to the other dataset. The best fitted relation can be derived as,

$$m = -0.69 \ln(d) + 4.929. \tag{4-18}$$

In the above relation, d is the separation distance between Tx and Rx nodes. This relation was employed during simulation to let the shape parameter vary with separation distance. Equation (4-18) and used data set is plotted in Fig. 4-2, where we can see depending on distance, the value of m parameter can fluctuate within the range of 0.16 to 5.8. As a result, for changing propagation distance the fading power envelope will also change.

4-3 Conclusion

In this chapter, different aspects of statistical channel modeling concepts for V2V communication were presented. Statistical models for multipath propagation were discussed extensively, providing their relevance with the presence of LoS component. To model more generalized multipath channel, Nakagami-m fading channel was illustrated and a relation was derived using linear regression on the mentioned empirical data set to vary parameter-m with changing Tx-Rx separation distance. It was also defined using autocorrelation function how velocity attribute for V2V communication can be implemented to represent signal level fluctuation due to vehicle mobility. Two most important conclusions from the discussions of this chapter are as follows,

- **for varying velocity of the vehicles the fading power spectrum can be calculated from V2V autocorrelation function presented by (4-11), and**
- **for varying Tx-Rx separation distance, Nakagami fading parameter-m can be calculated using (4-18)**.

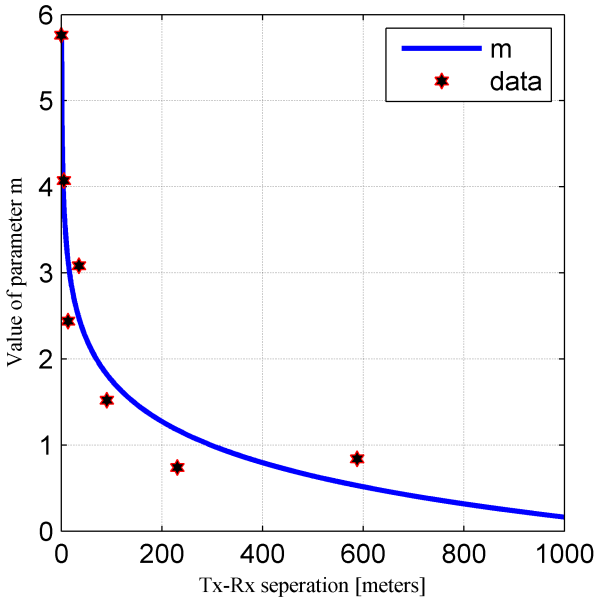

Figure 4-2: Relation of Nakagami-*m* parameter with distance.

How the Nakagami distributed fading envelope was mapped to the received signal strength will be discussed in the later chapter. The illustrated concepts were implemented for three different scenarios. For each scenario details simulation settings and results will be presented in the next chapter.

Chapter 5

Simulation of vehicular scenarios and results

5-1 Introduction

In the earlier chapters, details about the developed IEEE 802.11p node model and a realistic channel model for vehicle to vehicle communications were presented. It was shown, depending on the path loss exponents and standard deviation of signal fading derived from empirical measurements how different vehicular scenarios can be defined (e.g. suburban, urban, highway). For further realistic simulation settings, other parameters to characterize vehicular scenarios like simulating environment, vehicle density, velocity in the corresponding scenario, and interference due to multiple transmitters in the range will be outlined in this chapter. Then the simulation results specific to the scenarios will be presented and analyzed in the subsequent sections.

5-2 Simulation of suburban scenario

The location of the simulation scenario was taken as Hoofddorp which is a typical suburban area near Amsterdam, The Netherlands. The relevant attributes of the simulator is presented in Table. 5-1. In the simulated scenario 169 cars with IEEE 802.11p capability were distributed over total of 15 km length of road. Nevertheless, depending on the length and width of the roads, the density of the vehicles were 10 to 20 cars per square kilometers. Fig. 5-1 shows the initial distribution of the vehicles. The red cars were moving in the opposite direction as light blue cars on the same road. No lanes were considered though the roads were wide enough to overtake or cross one another. Each and every vehicle were assigned specific trajectory to follow a predefined path with varying velocity between 20-45 kilometers per hour. To keep the figure clutter free the trajectories are not shown in the plot. Cars were coming or moving away in burst due to lower speed limit and traffic lights in the suburban scenario. It is apparent that vehicle density depends on the time of the day. However, in our scenario the average value of vehicle distribution was considered. The same scenario was used to

Table 5-1: Simulator settings.

Attributes	Values
Frequency	5.850 GHz
Bandwidth	10 MHz
Transmit power	23 dBm
Antenna gain	0.0 dB
Data rate	6 Mbps
Packet format	MAC
Modulation	BPSK
Multiplexing	OFDM
Antenna height	1.51 m
Node velocity	20-45 Km/hr

run the simulator with other three different channel models like free space, two-ray, and already discussed empirical model for validation.

OPNET has 13 different pipeline stages to establish communication between a transmitter and multiple receivers. However, major concern of this research was how much power became available to the receivers. As a result, default power model which calculates received signal strength was replaced by Nakagami fading channel and proposed concepts. In the following subsections functionality of OPNET based transmitter and receiver pipeline stages will be presented.

5-2-1 Transmitter pipeline stages

In Fig. 3-7, Tx node attributes were presented, where six different pipeline stages for transmitter module can be found. In OPNET, it's only possible to program pipeline stages using *C* or *C++* programming languages. The used pipeline stages in the simulation scenario and their functionality are described below.

***rxgroup model*:** this attribute was set to *wlan_rxgroup* pipeline procedure which is able to determine connectivity between a Tx-Rx pairs. For example, a receiver in a different subnet rather than current Tx subnet should not hear to the transmitting node.

***txdel model*:** OPNET default transmission delay model is *wlan_txdel*. This model specifies the amount of time required to push all of the packet bits to the communication channel. This delay is proportional to the length of the packet (in bits).

***closure model*:** when Terrain Modeling Module (TMM) is not enabled all the vehicles will be considered as potential receivers of the messages. It is also possible to set a certain closure threshold. If path loss calculation depicts that signal strength will fall below the threshold then there will be no closure with associating receiver. However, in this study a closure model was programmed to limit the communication range within the 1000 meters (802.11p standard value).

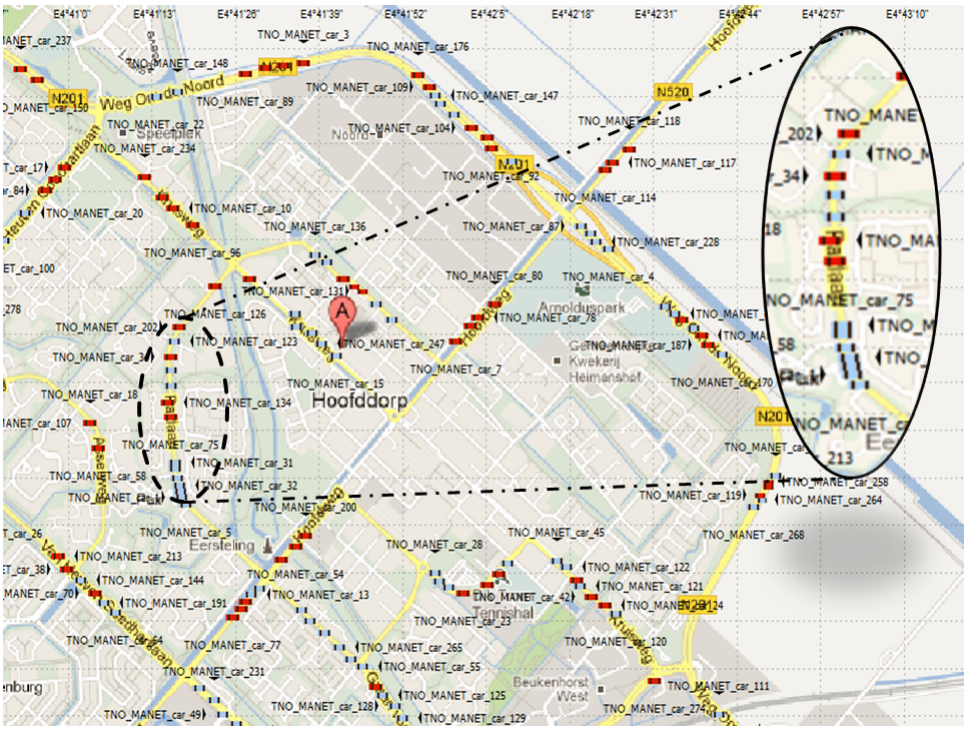

Figure 5-1: Suburban scenario with 169 mobile vehicles.

***channelmatch model*:** this pipeline procedure checks operating frequency, bandwidth, data rate, and modulation of the communicating transmitter and receiver. If the Tx, Rx frequency mismatches then corresponding packets will be considered as noise. Overlapping bandwidth of the two communicating nodes is used to determine in-band transmit power.

***tagain model*:** computes transmitter antenna gain. In this simulation study only omnidirectional antennas were considered which has gain of 1.

***propdel model*:** calculates end to end propagation delay based on Tx-Rx separation distance divided by speed of light.

5-2-2 Receiver pipeline stages

All the required receiver pipeline stages for calculating successful data reception along with their consequences for establishing communication will be discussed in this section. The outlined pipeline procedures in Fig. 3-8 are described below.

***ragain model*:** for particular incoming transmission this model calculates gain of the receiving antenna. Like Tx antenna Rx antenna gain was set to 1.

***power model*:** this is the most important pipeline stage for this research assignment as received signal strength is calculated by this pipeline stage procedure. It was already mentioned earlier sections that the proposed statistical channel model was programmed to be used as power model. In Fig. 3-8, we can see the model value for determining received power was set to *Nakagami_fading_channel*.

Table 5-2: Suburban scenario empirical parameters.

Parameter	Value
γ_1	2.1
γ_2	3.8
d_c	100

***bknoise model*:** this model is executed immediately after return of the received power stage to manipulate the effect of thermal noise.

***inoise model*:** this model calculates accumulated noise due to concurrent transmission by other transmitters within the range during a packet reception.

***snr model*:** pipeline procedure requires to calculate Signal to Noise Ratio (SNR) for detection of bits in the upcoming packets. The SNR model computes the noise ratio by adding all the interferences during the pk reception and the thermal noise. The SNR is then computed using the received in band transmit power and the total noise. The Signal to Interference and Noise Ratio (SINR) calculation will be discussed later in this chapter.

***ber model*:** *wlan_ber* was used to calculate Bit Error Rate (BER) on each packet segments based on previously computed effective SINR and modulation curve assigned to the receiver.

***ecc model*:** Acceptability of a packet is determined by this procedure. If number of bit errors in a packet exceeds threshold, the packet is rejected by this pipeline.

5-2-3 Suburban scenario: critical communication range

To implement large scale fading the Dual Slope Piecewise Linear (DSPL) model presented by (5-1) was programmed in *C++* to replace OPNET standard pipeline stage power model. Equation (5-1) differs from (2-5) by zero mean normally distributed random variables (i.e. X_{σ_1}, and X_{σ_2}) as small scale fading will be determined by statistical Nakagami-m fading model proposed in the earlier chapter. For simulating suburban scenario empirical DSPL parameters and corresponding values are listed in Table. 5-2.

$$p(d) = \begin{cases} p(d_0) - 10\gamma_1 log_{10}(\frac{d}{d_0}) & if\ d_0 \leq d \leq d_c \\ p(d_0) - 10\gamma_1 log_{10}(\frac{d_c}{d_0}) - 10\gamma_2 log_{10}(\frac{d}{d_c}) & if\ d > d_c. \end{cases} \tag{5-1}$$

The statistics obtained from the simulations were exported to MATLAB and reprocessed to accomplish better representation of the figures. In Fig. 5-2, the simulated result for large number of vehicles with empirical path loss model is presented, where it is clearly noticeable that simulated data resembles theoretical model. The figure depicts the vehicles can come as close as 0.3 meters due to their mobility over assigned trajectory. The critical distance which is expected to be 100 meters is also observable after that signal strength falls off rapidly due to greater path loss exponent. Furthermore,

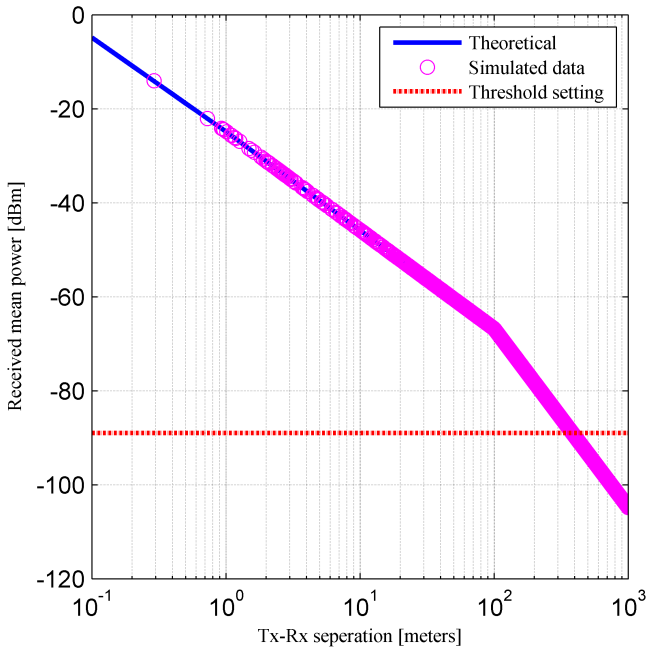

Figure 5-2: Simulated Dual Slope Piecewise Linear received mean power.

with the transmit power of 23 dBm the maximum attainable range of communication is roughly 386 meters though the IEEE amendment for 802.11p specifies allowable communication range of 1 km for Dedicated Short Range Communications (DSRC). The received power threshold was set to -89 dBm. The noise floor of the receiver is -104 dBm for a system with bandwidth of 10 MHz. The difference between threshold level and noise floor can be explained by taken into account noise figure and other system parameters like signal detection performance.

5-2-4 Suburban scenario: fading and Doppler effect

Vehicle to Vehicle (V2V) communication differs from cellular network because there is no fixed based station and vehicle velocities contribute Doppler effects to modulate the carrier frequency. The Doppler shift can have significant impact on signal fading. The time correlation property of the fading envelope was calculated using (4-11). Since, the power spectrum of the fading envelope is calculated from autocorrelation function, change in this correlation function has direct impact on signal level fluctuation of received signal. The Nakagami-m fading envelope described in previous chapter was applied over large scale path loss obtained using the DSPL model. The final equation which includes both the large and small scale fading is as follows,

$$p(d) = \begin{cases} p(d_0) - 10\gamma_1 log_{10}(\frac{d}{d_0}) + Z(m,\Omega) & if\ d_0 \leq d \leq d_c \\ p(d_0) - 10\gamma_1 log_{10}(\frac{d_c}{d_0}) - 10\gamma_2 log_{10}(\frac{d}{d_c}) + Z(m,\Omega) & if\ d > d_c. \end{cases} \tag{5-2}$$

where, $Z(m,\Omega)$ is Nakagami distributed with fading parameter m and shape parameter Ω. As a result, small scale fading was superimposed over large scale average received

power using (5-2). The empirical model parameters were discussed in Section 2-3-1-3. For the purpose of validation, the empirical model with measured parameters presented in [20] was used in the same suburban scenario. Then simulation data for empirical and realistic channel model was plotted in the same figure. In Fig. 5-3, we can see a good correspondence between amended Nakagami and the empirical model. At longer distances the difference increases. This is most probably due to sensitivity limit of the receiver (measurement) below which receiver could not detect signal anymore. Both of the models show critical distance at 100 meters. Signal fluctuation increases after this distance.

In Fig. 5-4, it is noticeable that with propagation distance the severity of fading increases. This is due to the fact, parameter m was varied with distance. Till about 300 meters the m parameter remained above the value of 1 (Fig. 4-2). As a result, within this range nearly no fading to Rician fading occurs. However, beyond 300 meters of separation distance m parameter becomes less than one. Consequently, harsher Rayleigh fading occurs beyond this distance when Line of Sight (LoS) component of the signal becomes less dominant which is also noticeable from the figure. In the case of suburban scenario, due to low density of vehicles it is evident that LoS component will be present in nearby distances. However, with increasing distance more multipath components will appear owing to reflections from buildings and scattering environment in the vicinity of roads. Fig. 5-4 explains these real life multipath propagation anomalies and shows the proposed method can represent these phenomena. Critical distance at 100 meters is visible within which signal strength fluctuates without crossing the threshold. Nevertheless, Packet Error Rate (PER) will increase substantially beyond 100 meters for the threshold setting of -89 dBm. To compensate this problem transmit power or receiver sensitivity needs to be increased.

5-2-5 Suburban scenario: Signal to Interference and Noise Ratio (SINR)

To address interference caused by multiple transmitters in the range SINR can be defined as,

$$SINR = \frac{P}{N + I}\,, \tag{5-3}$$

where, P is the received power, N is the receiver's back ground noise, and I is the accumulated interference noise contributed by simultaneous transmissions within the range. In Fig. 5-5, retrieved SINR values for four different channel models simulated in the same suburban scenario are presented. The SINR values were calculated using (5-3) during simulation. Then time averages of samples were derived within 3 second bins to plot the figure which made it easier to interpret the result. From Fig. 5-5, it can be observed that there is an difference of about 20 dB between SINR retrieved using free space Propagation model and proposed realistic channel model. Whereas, marginal differences were obtained between free space propagation and two-ray model. Nevertheless, the proposed channel model showed less discrepancy (6 dB) with the empirical channel model. This 6 dB SNR can be explained by the fact at longer distances higher attenuated signals were not included in the empirical model. Compared to free space and two ray model, Nakagami channel model and empirical channel model showed

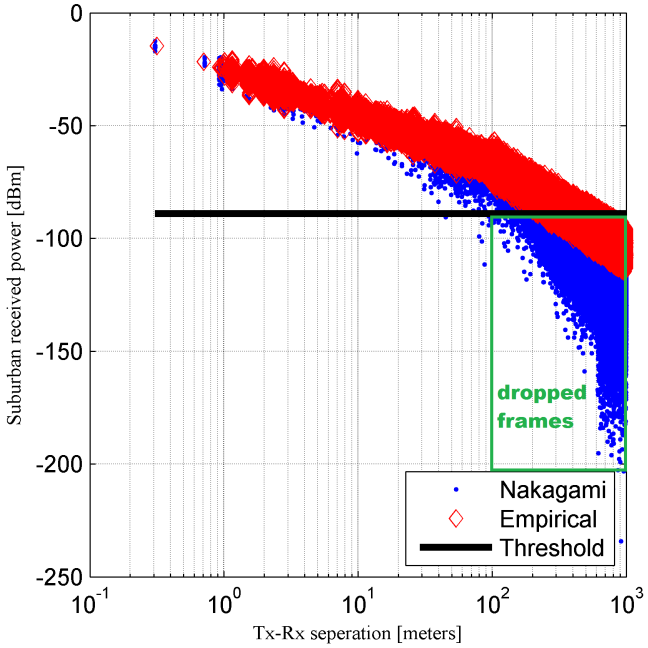

Figure 5-3: Suburban received power: Nakagami and empirical channel model.

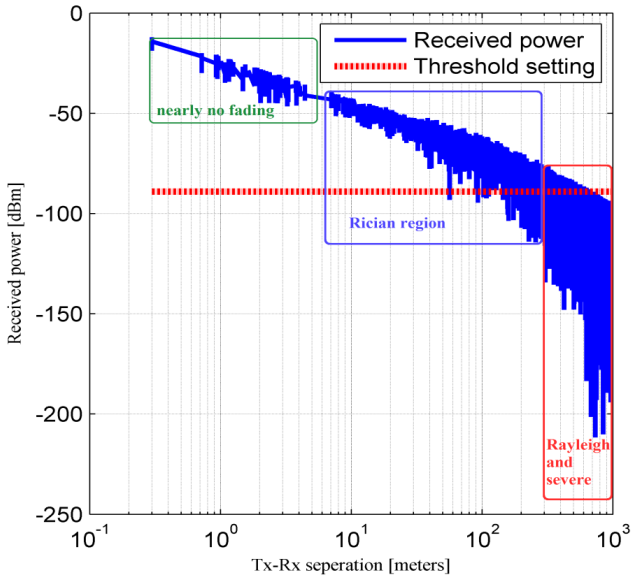

Figure 5-4: Simulated received power over propagation distance.

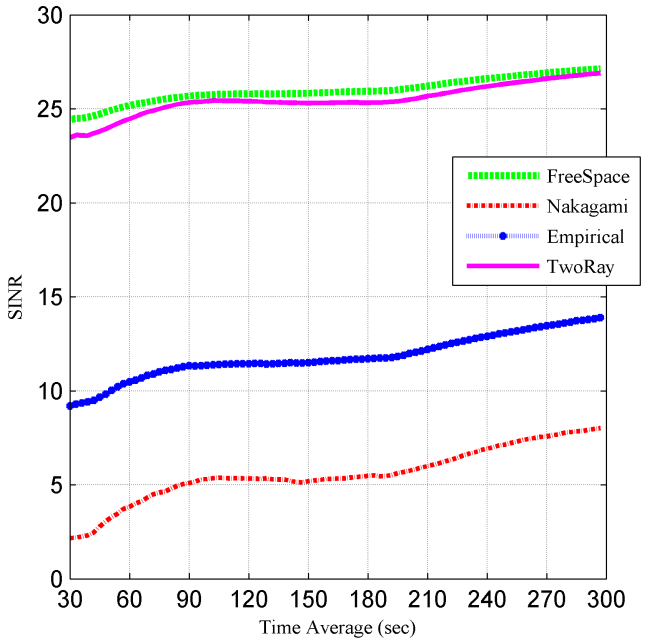

Figure 5-5: SINR for four different channel models.

heavily fluctuating SINR in the receiver (not shown in Fig. 5-5). Identical behaviour was found for the empirical model. This might occur due to presence of multipath components of the signal and varying Doppler frequency imposed by Tx-Rx velocity which is evident for V2V communication.

5-2-6 Suburban scenario: Bit Error Rate (BER)

As expected, Fig. 5-6 shows similarity in between simulated Nakagami model and the empirical model. Marginal difference was found among the two models which reveals accuracy of the proposed model. During the whole simulation time, out of 1000 bits roughly 1 bit was received in error by the receiver. On the other hand, free space and two-ray model showed identical BER as they returned similar SINR. The BER was slightly decreasing which might be due to less number of interfering mobile nodes or decreasing Tx-Rx separation distance. From the consequences of Fig. 5-6, it can be deduced that depending on the complexity of the model or the used method to develop the model can greatly influence obtained simulation results as there is a factor of 10 difference in the BER curves between empirical and free space or two-ray model.

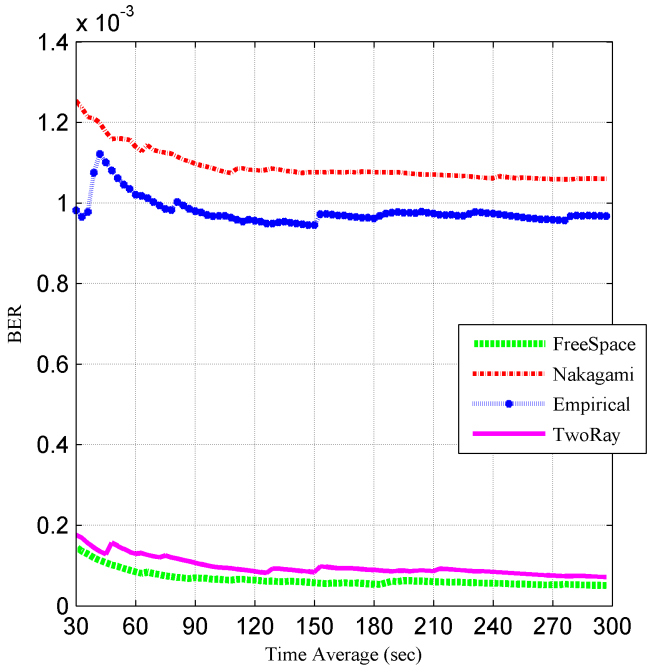

Figure 5-6: Suburban scenario Bit Error Rate.

5-3 Simulation of highway scenario

In Fig. 5-7, we can see the simulated highway scenario. The location was chosen as the highway in between Helmond and Eindhoven which is being used in the Netherlands to test and develop Intelligent Transportation Systems (ITS) applications. In this case, vehicle velocity was assigned from 80 to 100 Km/hr which is higher than suburban scenario. Total length of the road was roughly 20 km. 200 mobile vehicles were distributed over the mentioned length of road. Two road lanes and no road traffic signals were considered. As a result, vehicles were randomly distributed over the highway. The red cars were moving in the opposite direction as white cars on the same road in different lanes. All other physical layer parameters and used pipeline stages remained same. Like suburban scenario, numbers of channel models were used to generate statistics for this highway scenario.

5-3-1 Highway scenario: critical communication range

For the simulation of highway scenario DSPL empirical parameters were retrieved from [21]. The critical distance, and path loss exponents are presented in Table. 5-3. In the table, we can see smaller values of path loss exponents compared to suburban scenario. This is due to the fact that there are fewer pedestrians and less number of near by obstacles in the highways. As a result, the signal is less likely to be reflected by objects above the ground (e.g. buildings, trees, hills) [20]. These parameters were invoked in (5-1) to calculate large scale fading for the simulation scenario. In Fig. 5-8, again we can see very good agreement in between simulated data and theoretical

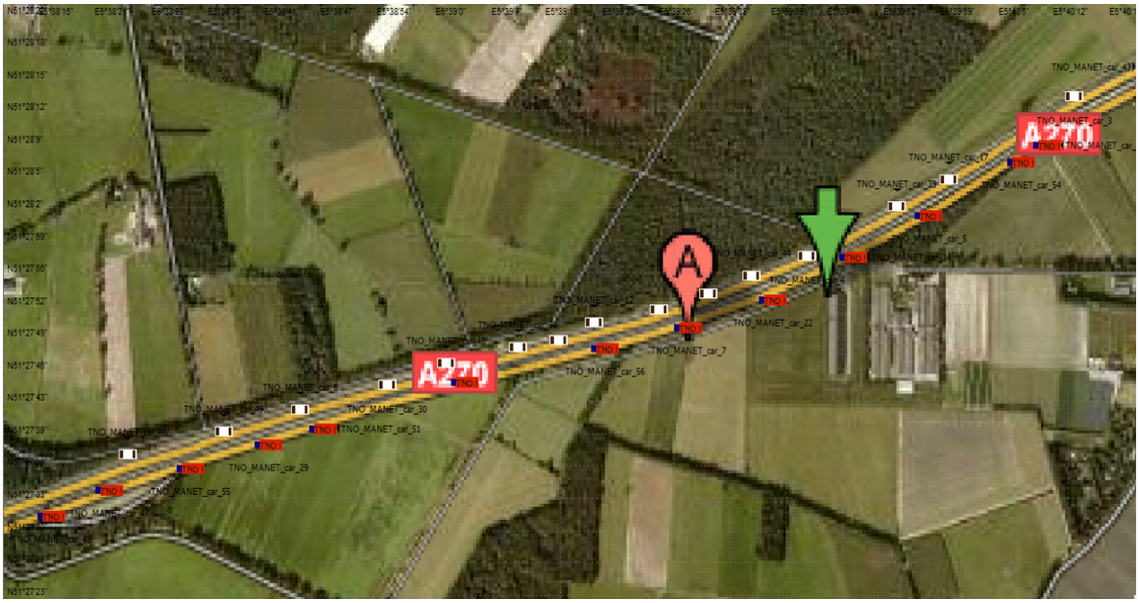

Figure 5-7: Highway scenario with 169 IEEE 802.11p nodes.

Table 5-3: Highway scenario empirical parameters.

Parameter	Value
γ_1	1.9
γ_2	4
d_c	220

DSPL model for the given parameters. As expected, the critical communication range is visible at 220 meters. For the threshold setting of -89 dBm, the maximum attainable communication range is roughly 550 meters which is a much higher range compared to suburban scenario due to presence of less number of scatterers.

5-3-2 Highway scenario: fading and Doppler effect

For the simulation of highway scenario, (5-2) was used along with empirical path loss parameters presented in Table. 5-3. Again, Nakagami fading was superimposed over large scale DSPL fading power. For the sake of validation both the proposed realistic channel model and empirical model presented in [21] was plotted in the same figure. The dual slope empirical path loss parameters and standard deviation σ_1 and σ_2 for highway scenario were presented in Table. 2-5. The obtained results are presented in Fig. 5-9 where we can see good accordance between the proposed Nakagami channel and empirical channel. In the scatter figure, at 220 meters the critical distance is visible for both of the models after which fading increases rapidly. However, at larger distances the difference between the two models increases. This can be due to the fact that the empirical measurement was taken till 588 meters [20]. Another reason can be the packets were already dropped in the measurement due to very weak signal strength (at the receiver) at larger distances, which is also very logical as we can see signal

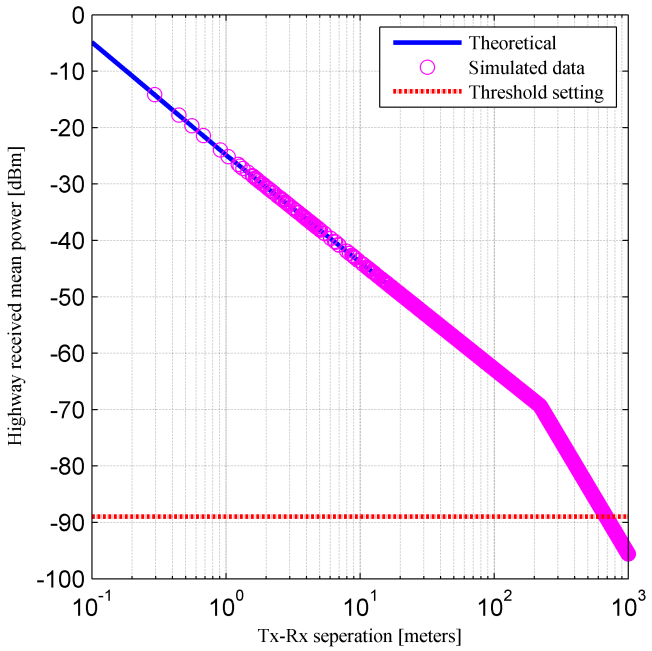

Figure 5-8: Highway scenario received mean power.

strength already decaying below threshold beyond 200 meters. In Fig. 5-10, the result obtained with the Nakagami channel model was plotted. It is noticeable from the figure that the Rician region for highway scenario is quite long compared to that of suburban scenario presented in Fig. 5-4. This is an interesting result. The reasons for long Rician region are very small number of nearby obstacles, cars were distributed on more of one dimensional road, and highways are straight enough to maintain direct line of sight component between transmitter and receiver. However, due to higher transmitter and receiver velocity it is evident that the signal level fluctuation will be higher on highways compared to the suburban scenario which is also visible in the figure. Another key result that can be interpreted from the figure is, after Rician region the multipath components interfere each other only destructively. Hence, in the Rayleigh and severe fading region signal falls off abruptly.

5-3-3 Highway scenario: SINR and BER

Numbers of different channel models were used in the simulations for the same highway scenario. Then the data was exported to MATLAB to draw figures. For SINR and BER similar difference in between empirical and proposed channel model was found. As BER is the final result determined by SINR value, for highway and rural scenarios only BER results will be discussed. In Fig. 5-11, the BER curves are presented for different channel models. All the used models showed better BER performance compared to suburban scenario (Fig. 5-6) due to their higher SINR values. DSPL path loss parameters and critical distance for highway scenario were close to two-ray parameters. Again marginal difference in between empirical and Nakagmi channel was found which reveals

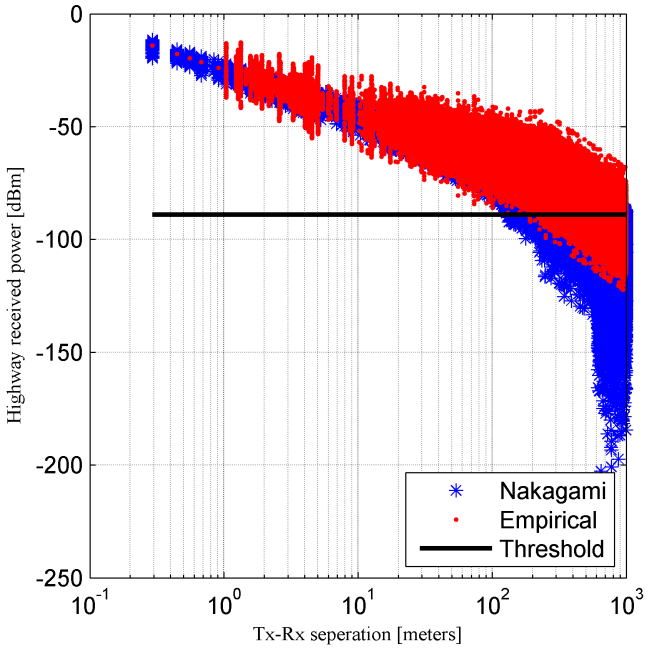

Figure 5-9: Highway received power: Nakagami and empirical channel model.

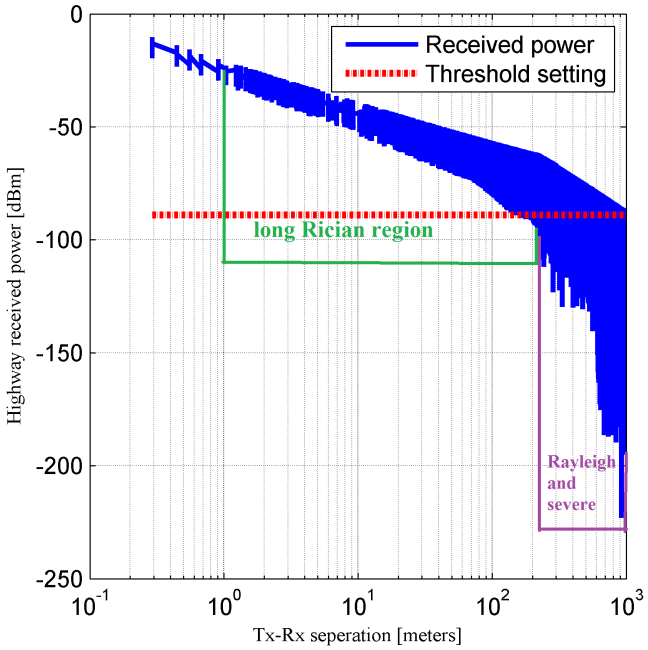

Figure 5-10: Highway scenario received power using Nakagami channel model.

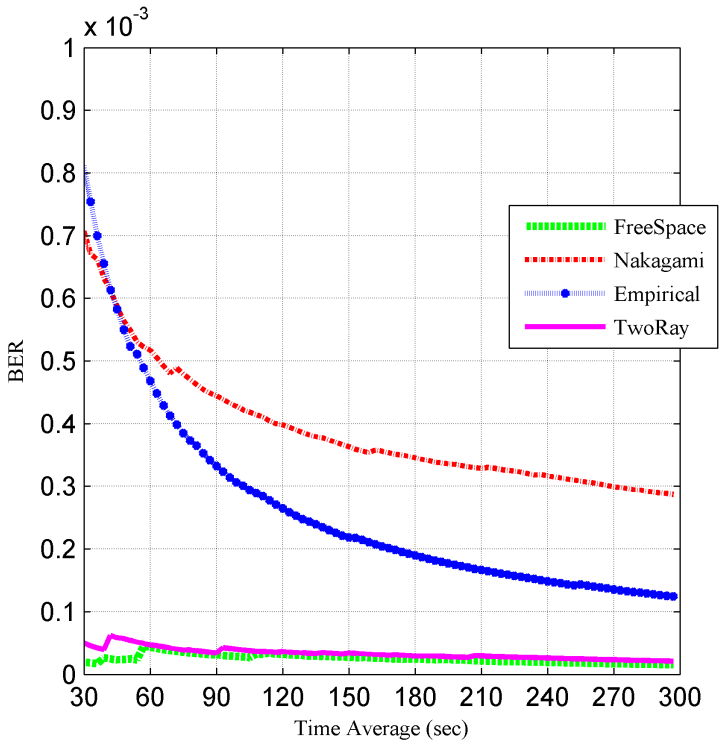

Figure 5-11: Highway scenario Bit Error Rate.

reasonable accuracy of the proposed channel model. With increasing simulation time the BER decreases for all four cases, this is due to the redistribution of vehicles on their trajectories during simulation and less number of interfering nodes available within the range.

5-4 Simulation of rural scenario

Rural scenario is partially comparable with highway scenario as speed limit is roughly 40 Km/hr to 80 Km/hr. In the local areas, there are small buildings, trees, hills, and crop fields. The rural scenario was chosen as Loosduinen which is a typical rural area nearby The Hague. In Fig. 5-12, we can see the simulated rural scenario. No lanes were considered. However, roads are mainly 2-way streets. Total of 200 vehicles were distributed over 30 kilometers length of road. Like the previously discussed suburban and highway scenarios, rural scenario was simulated for numbers of channel models for collecting statistics.

5-4-1 Rural scenario: critical communication range

Similar to the other two scenarios large scale fading was calculated using empirical DSPL path loss parameters. The parameters are listed in Table. 5-4. The table shows that rural scenario critical distance is 226 meters compared to 220 meters and 100 meters for highway and suburban scenarios respectively. The first path loss exponent

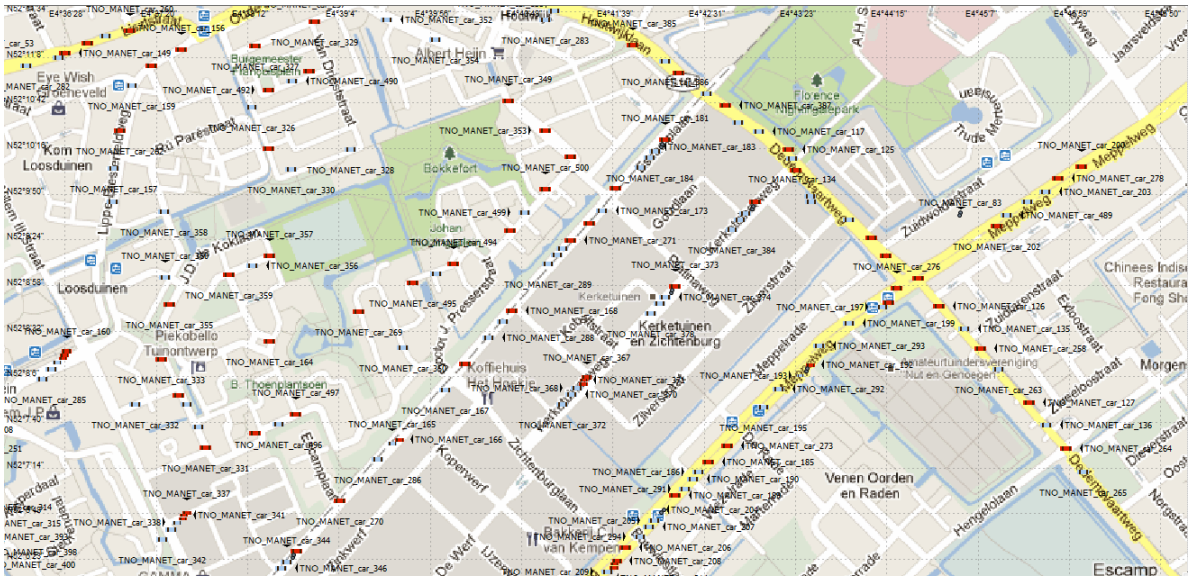

Figure 5-12: Rural simulation scenario with mobile vehicles.

Table 5-4: Rural scenario empirical path loss parameters.

Parameter	Value
γ_1	2.3
γ_2	4
d_c	226

γ_1 has a higher value than highway scenario due the to presence of small buildings and scatterers like vegetation or trees in the vicinity of the roads. After the critical distance d_c the second path loss exponent γ_2 has the same value as in the highway scenario. These values were used in the pipeline stage to define large scale fading. In Fig. 5-13, we can see the retrieved simulation data is in agreement with the theoretical DSPL model. The critical distance is visible around 226 meters and subsequently the model is validated. After the critical distance the signal level drops off more abruptly due to the higher path loss exponent. For the threshold setting of -89 dBm the maximum possible vehicle to vehicle communication range in rural areas is 400 meters which is shorter in contrast to 550 meters of highway scenario. This is logical due to the fact that unlike highway scenario, in rural scenario roads may not be straight enough or more number of scatters are present to obstruct LoS component in larger distances.

5-4-2 Rural scenario: multipath fading and Doppler spread

For the purpose of validation the proposed realistic channel and empirical model with parameters presented in [21] were simulated in the same rural scenario. In Fig. 5-14, we can see the received power obtained using Nakagami channel resembles with the empirical model. However, at larger distances the difference increases which can be explained by the fact that measurements for deriving the empirical parameters were taken only for one transmitter and one receiver. Moreover, the channel was measured till

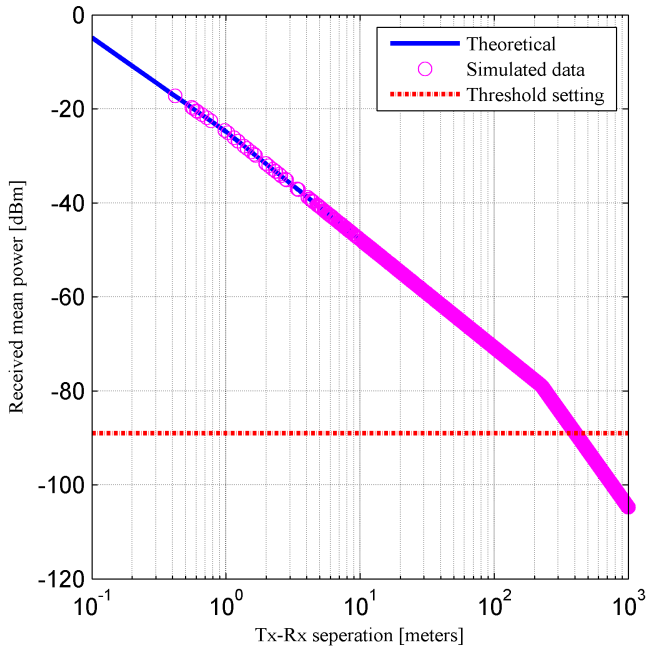

Figure 5-13: Simulated received mean power for the rural scenario.

588 meters (maximum). As a result, interference due to other transmitters were totally absent. It is evident that, for increasing distance the probability of more interfering nodes will increase along with already discussed multipath scatterers. For more clear presentation the same figure is presented in Fig. 5-15 where we can see similar result as highway scenario. It is noticeable from the figure that less fluctuation of signal strength was achieved in case of rural scenario due to lower speed limit compared to highway scenario. However, due to occupancy of more multipath scatterers in the vicinity of roads the signal level drops off quickly which was also found in the Fig. 5-13. Critical distance is visible around 226 meters after which heavily fluctuating signal fading occurs. Again long Rician region identical to highway scenario is noticeable in the figure. This is due to less number of traffic on the streets and smaller number of obstacles compared to suburban roads.

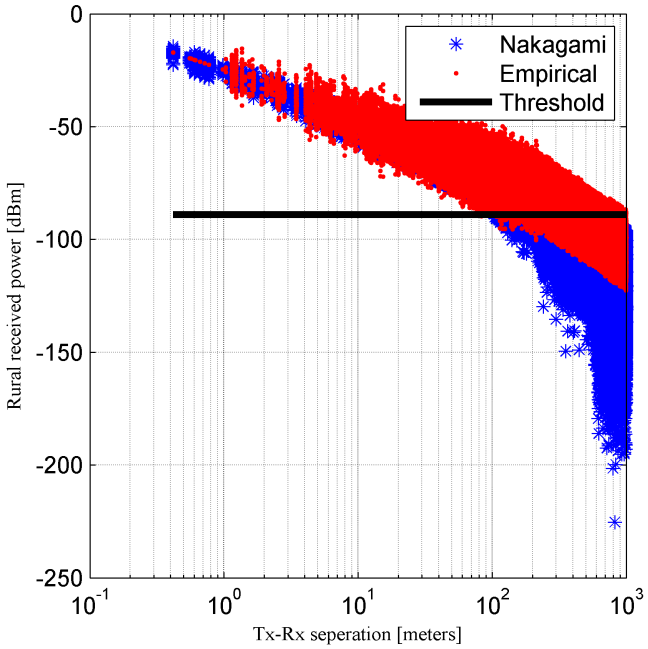

Figure 5-14: Rural received power: Nakagami and empirical channel model.

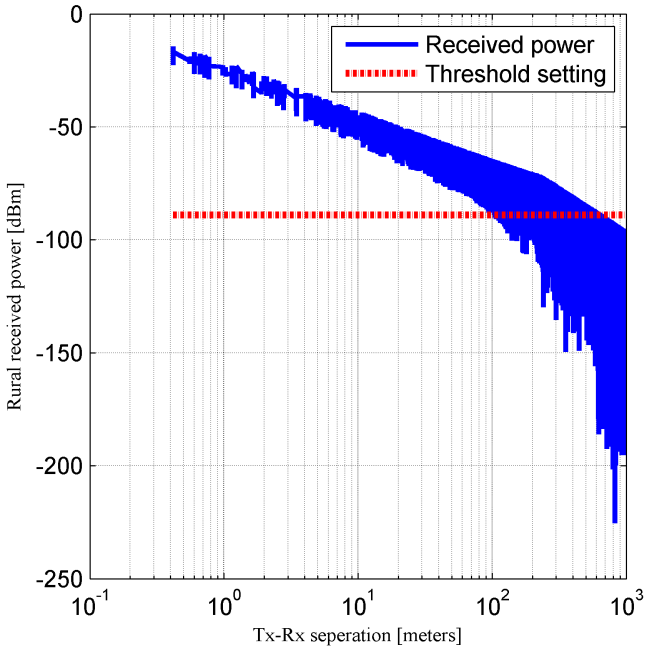

Figure 5-15: Rural scenario received power using Nakagami channel.

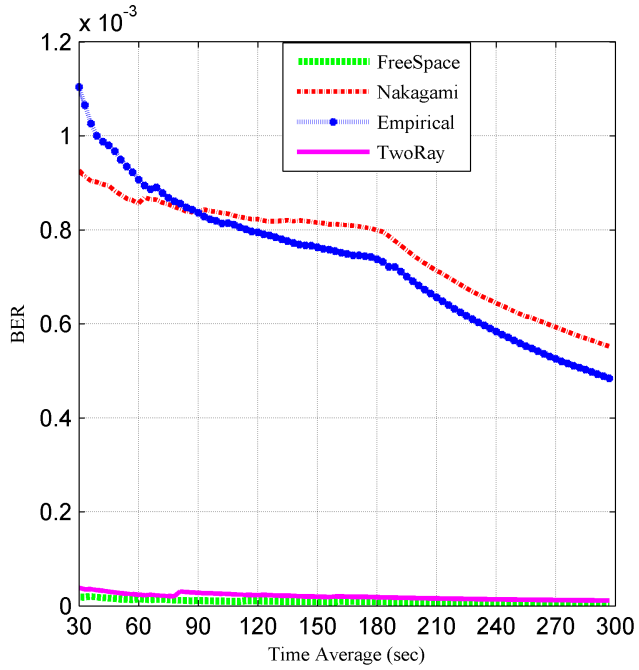

Figure 5-16: Rural scenario Bit Error Rate.

5-4-3 Rural scenario: Bit Error Rate (BER)

As expected, in Fig. 5-16 the BER curves obtained using realistic channel and empirical model show very fine resemblance. Both the cases out of 1000 bits there is possibility that one bit will be received in error. In contrary, optimistic result are obtained when using two-ray and free space propagation models. Much less bit errors were obtained using later two models and differences observed with empirical or Nakagami model are a factor of 100. We have seen similar results for highway scenario.

5-5 Comparison between different scenarios

In this Section, results obtained from suburban, highway, and rural scenarios in earlier part of the chapter will be compared. In Fig. 5-17, attenuation of signal strength considering large scale fading is presented for the three different scenarios. Since, rural scenario has highest path loss exponent γ_1 of 2.3, till corresponding critical distance the signal decayed quicker than other two scenarios. Though suburban and highway scenarios have identical path loss exponents (Table. 2-5) former has longer critical distance of 220 meters. As a result, among the three scenarios highway scenario has obtained longer communication range. Due to presence of more buildings, trees, and vehicles compared to other two scenarios minimum communication range was attained for the suburban scenario. However, suburban and rural scenario showed comparable result.

Multipath fading and Doppler spread for the suburban, highway, and rural scenarios were discussed in their respective sections. Fig. 5-18 depicts few interesting results concerning multipath and Doppler in the three different scenarios. It is noticeable from

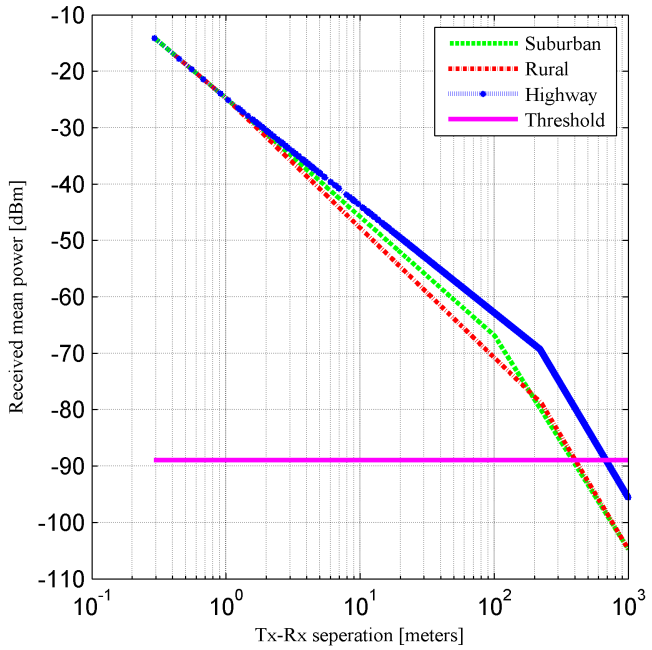

Figure 5-17: Large scale signal attenuation for the three scenarios.

the figure that for suburban scenario signal level falls off quickly and fluctuates with higher magnitude at longer distances compared to rural and highway scenario. This is because of higher density of buildings and scatterers that contribute to a higher number of multipath components. With increasing distance more scattered replicas of the signal arrive at the receiver. For the rural scenario the signal strength varied less than that in the suburban scenario. Nevertheless, due to hills, trees, and houses in the rural areas the signal strength should fall more quickly than that in the highway scenario which is also noticeable from the figure. In Section 5-3-2, it was explained that at higher velocity, spread of signal level fluctuation increases. It was also explained how LoS component significantly improves communication range and performance on highways. However, one key observation can be deduced comparing all the three scenarios presented in Fig. 5-18 is, multipath fading is more deciding factor for communication quality compared to Doppler effect. The same conclusion was found for satellite or cellular communication.

5-6 Effect of interference due to number of vehicles in the range

To analyze effect of vehicle density on BER, already presented highway scenario was simulated using 10, 20, 60, 100, and 200 nodes including the realistic channel model. To keep the network area constant vehicles were distributed on a horizontal line of 1000 meters for all the cases. This is to increase vehicle density within the same highway with increasing numbers of mobile nodes and to maintain standard communication range for DSRC. Then simulation was run using 10, 20, 60, 100, and 200 vehicles in the same area. In the Fig. 5-19, we can see considerable difference of BER for different

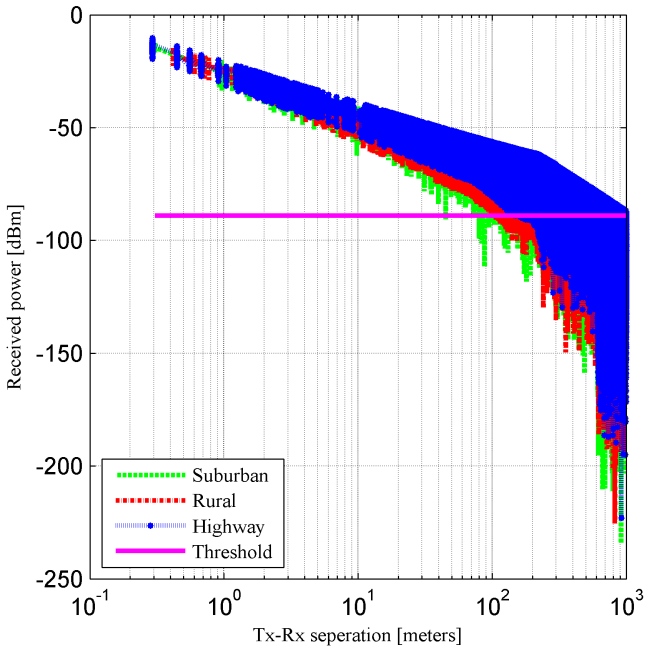

Figure 5-18: Received power using Nakagami channel for the three scenarios.

vehicle density. With increasing vehicle density BER rate increases rapidly. As already discussed before, interference due to other concurrent transmission was included for SINR calculation. As a result, for greater number of transmitters in the range BER increases proportionally.

5-7 Convergence of simulation time

For any kind of simulation study it is always a greater concern whether the simulation time is sufficiently long enough so that the time average statistical results are converged. To answer this question, the Hoofdorp scenario was executed for five different simulation time of 3 minutes, 4 minutes, 5 minutes, 10 minutes, and 15 minutes with the same Nakagami channel. In Fig. 5-20, the cumulative distribution of BER extracted from the different simulation run are presented where we can see probability of bit errors for the mentioned set of simulation time reasonably converges. It should be noted that in this study all the results were retrieved from 5 minutes of simulation time as longer simulation time was consuming unusually greater amount of time.

5-8 Discussions

There are numbers of contributions in the literature where large scale path loss model parameters and small scale fading were determined based on empirical measurements using DSRC radios. Most of the cases just one transmitter and one receiver was used for the measurement. For large scale network no data was found. For different

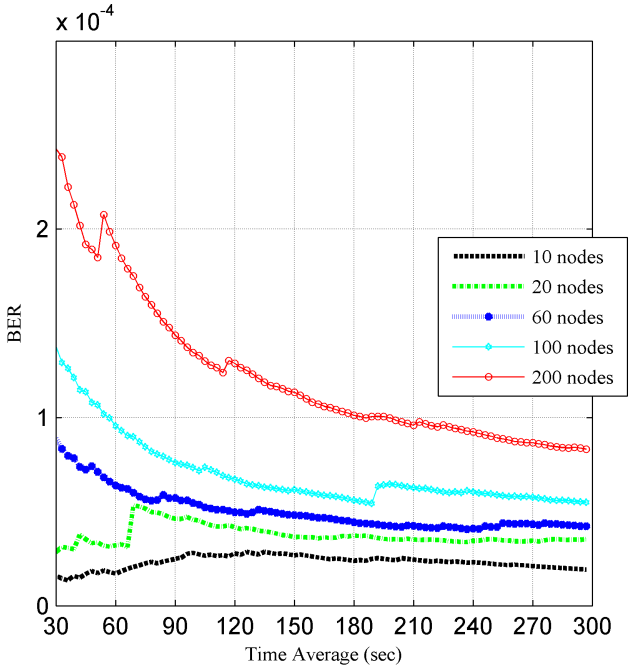

Figure 5-19: BER for different vehicle densities.

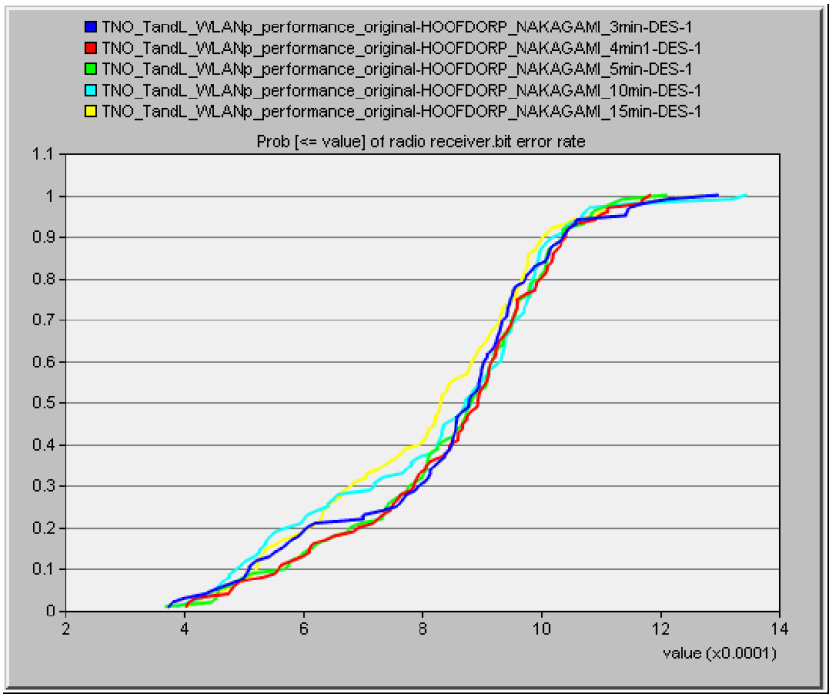

Figure 5-20: Cumulative distribution of BER for different simulation time.

measurement campaigns significant difference between measured path loss exponents and critical distance were observed. As a result, the most consistent model parameters (for three scenarios) provided by Lin Cheng was used in this research for modeling and validation. Surprisingly, urban scenario for V2V communication was hardly measured and unrealistic path loss exponents and critical distance were observed in the literature.

OPNET is a powerful network simulator which supports both object oriented programming of models and Discrete Event Simulation (DES). Since, it works based on discrete sequence of events, the simulation runs faster than continuous simulation. Few of the clear advantages of OPNET over other network simulators are Graphical User Interface, programmability of the models, very rich libraries with recent network protocols and technologies. Moreover, the hierarchical modeling in OPNET enables modeling and simulation task easy to manage. Graphical User Interface based tracing and debugging provides a convenient way to troubleshoot bugs in the models. Real-time simulation messages and updates render users to monitor progress and status of the simulation run. However, author has found few shortcomings and challenges very difficult to accomplish during simulation of the presented concepts. Rest of this section will be devoted to address those problems and possible solutions.

***OPNET installation*:** Initially it look quite bit of time to correctly run the Modeler as for different Windows Operating System (OS) different versions of OPNET Modeler is compatible. Before installing Modeler an already installed *C/C++* compiler should be in the system as OPNET installation package does not have a default compiler engine. Microsoft Visual Studio (MSVS) could be a good option. Again, appropriate version for the respective OS should be chosen. When finished with both the MSVS and Modeler proper system environment variables must be set to execute the program properly.

Solution: Author has found MSVS 2010/2008 compiler is compatible with OPNET Modeler 14.5 and later versions for Windows 7/8 (64/32 bits) operating systems. For different versions of the compiler different environment path variables should be found in the OPNET web-site.

***Licensing*:** OPNET is an expensive commercial software. As a result, license is required to get access to model libraries or to run the simulator. For getting access to a floating license from a license server both the server and the workstation should be in the same subnet platform. At the beginning, it took much effort to get the license from the server. Misleading messages from license management window were appearing without any proper guideline.

Solution: To easily get access to the license server inbound rules for Windows firewall and installed antivirus software solved the problem. License port should be turned on before start of the Modeler in the workstation. Some cases license files were shown but they were inaccessible.

***Compatibility of models*:** One of the surprising shortcomings of this simulation platform is models developed using OPNET Modeler 14.5 or earlier versions of the software may not be usable in the latest versions of the simulator.

Solution: For this particular problem no method was found except developing models in the new version or installing respective congenial older version.

***External* C/C++ *library*:** For generating Nakagami-m fading channel it was required to use external *C++* libraries. OPNET does not posses built in functions or libraries to generate complex numbers, Fast Fourier Transform (FFT), vector containers, or function to calculate variance of the signal. Moreover, it was required to use Bessel function and to generate normally distributed random numbers. Though OPNET has random number engine and different distributions when those were being used in a loop, no events were generated.

Solution: Using MSVS 2010 complex numbers, vector containers, Bessel function, and different distributions were accessed or generated. In [36], a very good library was included with all the required functions (e.g. FFT, inverse FFT, variance) which enables to program pipeline stages like in *C/C++* editor. It should be noted that before using the library all the header files and library files should be included in MSVS library, bin, and include directories.

***Mobility*:** Mobility is the most important property of vehicle to vehicle communication. As already discussed, OPNET mobility models can be directly used in the simulation scenarios. For specific mobility definition trajectories were used instead of random mobility. The trajectory velocity information was necessary in the power model pipeline stage to calculate autocorrelation function or signal level fluctuation. At the beginning, no easier way to retrieve the mentioned trajectory attribute was found. This is at least not properly explained in OPNET product documentation.

Solution: Trajectory information can be accessed using,
op_ima_traj_info_get(node id (Tx or Rx), start time, speed, ascent rate of the node, end time)
simulation kernel. Author has found during setting up different scenarios, this kernel provides greater freedom to implement mobility in pipeline as based on Tx or Rx node id velocity information can be directly obtained from the kernel.

Chapter 6

Conclusions and future works

Major research goals of this graduation project were to thrive realistic channel models for different Vehicle to Vehicle (V2V) communication scenarios, and to test vehicular empirical channel models in large scale simulation platforms for those scenarios. Endeavor was put forth for the IEEE 802.11p node model and for maintaining feasibility of the results so that outcome of this research can be implemented in the real life applications. Since, the results will be applied to Java Intelligent Transportation Systems (ITS) modeler currently being developed by Netherlands Organization for Applied Scientific Research (TNO), scalability of the communication range with different level of signal fading (e.g. Rician, Rayleigh) was examined.

At the beginning, literature survey showed almost all the large scale simulation contributions were based on overly optimistic free space, and two-ray propagation channel models. Few of them studied Wireless Access in Vehicular Environments (WAVE) using large scale Ad-Hoc network node models due to unavailability of the 802.11p node model in the network simulators. As a result, to an extend this study represents more realistic large scale simulation of vehicular network employing the standard in the node model. In Chapter 3, necessary architectures, modules, and attributes of the node model relevant to this project were outlined.

Critical communication range for suburban, highway, and rural scenarios were examined considering large scale path loss only. The scenarios were defined based on empirical pathloss parameters and variance of signal strength. Comparison showed, suburban scenario range of communication is minimum among the three. This is due to presence of more number of buildings, trees, and vehicles on suburban roads compared to other two scenarios. In Table. 6-1, a rough sketch of obtained communication ranges for those scenarios are presented.

Small scale fading for V2V scenario was defined in Chapter 4. Since, communicating vehicles are in motion, a well known model of autocorrelation function which employs both Tx and Rx velocity was explained in the chapter. Using three different Tx-Rx velocity pairs it was illustrated how increasing Doppler frequency can affect power spectrum and increase signal fluctuation.

A novel idea was presented in this thesis which comprised signal fading with trans-

Table 6-1: Communication range.

Scenario	Range (meters)
Suburban	386
Highway	550
Rural	395

mitter and receiver separation distance. It was shown how varying propagation environment was mapped to signal fading using Nakagami-m parameter. As an example, for suburban scenario roughly till 300 meters nearly no fading to Rician fading occurred. Beyond this distance when LoS component of the signal became rarely available Rayleigh fading to more severe fading were observed.

Initially, four different channel models were compared (i.e. free space, two-ray, empirical, Nakagami). The analysis showed, overly simplified model for the mentioned use case may imply optimistic results which were unrepresentative of the original propagation anomalies. The proposed realistic model resembled with the empirical channel model. The empirical channel model showed marginally less Bit Error Rate (BER) than the presented realistic channel model. This may be because of the model was developed taking measurements for less Tx-Rx separation distance than that of this study and with one transmitter and one receiver only. As a result, interference due to other transmitters were not included. It was found in Fig. 5-19 that for increasing vehicle density BER increases.

When multipath fading and Doppler effect was applied to signal fading, it was noticed, in suburban scenario signal level falls off quickly at longer distances compared to rural and highway scenarios. The increased BER was observed in suburban scenario due to lower Signal to Interference and Noise Ratio (SINR) values. Average spread of signal level fluctuation was greater on highways. However, comparison showed suburban scenario communication range is shorter and due lower mean signal strength communication performance was lessened compared to other two scenarios. The key conclusion which can be deduced comparing all the three scenarios is, the multipath fading is more deciding factor for communication quality compared to Doppler effect.

The presented realistic channel model not only can be used for representing underlying propagation environment for any sort of mobile communications but also for large scale simulation and performance evaluation of higher layer protocols for ITS applications.

6-1 Future works

The introduced concepts in this thesis will be implemented in Java ITS Modeler simulator where performance of the vehicular network and applications will be analyzed before real life implementation. Effort will be given to study Medium Access Control (MAC) layer and upper MAC layer protocols. For innovative applications of ITS further research will be done in the near future. In case of urban scenario, surprising inconsistency was found in the derived empirical parameters presented in the literature

compared to other three scenarios. As a result, an empirical study will be carried out in my future studies to determine realistic urban scenario channel parameters.

Bibliography

[1] "Part 11: Wireless LAN Medium Access Control (MAC) and Physical Layer (PHY) specifications,"IEEE std. 802.11, June 2007.

[2] D. Jiang, L. Delgrossi, "IEEE 802.11p: Towards an International Standard for Wireless Access in Vehicular Environments," *IEEE Vehicular Technology Conference*, pp. 2036-2040, May 2008.

[3] "IEEE Standard for Wireless Access in Vehicular Environments (WAVE) Multichannel Operation", IEEE std. 802.11p, February 2011.

[4] "IEEE Standard for Wireless Access in Vehicular Environments (WAVE) Networking Services", IEEE std. 802.11p, December 2010.

[5] "IEEE Trial-Use Standard for Wireless Access in Vehicular Environments-Security Services for Applications and Management Messages", IEEE std. 802.11p, July 2006.

[6] A. Jamalipour, "Cognitive Heterogeneous Mobile Networks," *IEEE Trans. on Wireless Comm.*, pp. 2-3, June 2008.

[7] "Commision decision on the harmonised use of radio spectrum in the 5875-5905 MHz frequency band for safety-related applications of Intelligent Transport Systems (ITS)." ETSI std, 2008/671/EC, August 2008.

[8] V. Shivaldova, "Implementation of IEEE 802.11p Physical Layer Model in SIMULINK," Technischen Universitat Wien, July 2010.

[9] M. Muller, "WLAN 802.11p Measurements for Vehicle to Vehicle (V2V) DSRC", September, 2009.

[10] "Wireless LAN Medium Access Control (MAC) and Physical Layer (PHY) specifications Amendment 8: Medium Access Control (MAC) Quality of Service Enhancements," IEEE Std. 802.11e, Nov. 2005.

[11] "Local and metropolitan area networks– Specific requirements– Part 11: Wireless LAN Medium Access Control (MAC) and Physical Layer (PHY) Specifications Amendment 6: Wireless Access in Vehicular Environments", IEEE Standard 802.11p, July, 2010.

[12] K. Bilstrup, E. Uhlemann, E. G. StrÃűm, and U. Bilstrup,"Evaluation of the IEEE 802.11p MAC method for Vehicle-to-Vehicle Communication,"*IEEE Vehicular Technology Conference*, pp. 1-5, September 2008.

[13] E. G. Strom, "On Medium Access and Physical Layer Standards for Cooperative Intelligent Transport Systems in Europe,"*IEEE Proceedings*, Vol. 99, No.7, pp 1183 - 1188, July 2011.

[14] C. Cseh, "Architecture of the dedicated short-range communications (DSRC) protocol," *in Proc. 48th IEEE Vehicular Technology Conf. (VTC)*, 98, vol. 3, pp. 2095 - 2099, 1998.

[15] ETSI, Document EN 302 665, "Intelligent Transport Systems (ITS); Communication Architecture," Sept. 2010. Version 1.1.1.

[16] "Intelligent Transport Systems (ITS); European Profile Standard for the Physical and Medium Access Control Layer of Intelligent Transport Systems Operating in the 5 GHz Frequency Band," ETSI ES 202 663 (V1.1.0).

[17] W. R. Braun, U. Dersch, "A Physical Mobile Radio Channel Model,"*in IEEE Transactions on Vehicular Technology*, VOL. 40, NO. 2, MAY 1991.

[18] Andrea Goldsmith, Wireless Communications. New York : Cambridge University Press, 2005.

[19] T.S Rappaport, Wireless Communications: Principles and Practice, 2nd Edition, Prentice Hall, 2002.

[20] L. Cheng, B. Henty, D. Stancil, F. Bai and P. Mudalige,"Mobile vehicle-to-vehicle narrow-band channel measurement and characterization of the 5.9 GHz dedicated short range communication (DSRC) frequency band,"in *IEEE Journal on Selected Areas in Communications*, vol. 25, no. 8, pp. 1501 — 1516, 2007.

[21] L. Cheng, B.E. Henty, F. Bai, and D. D. Stancil, "Highway and Rural Propagation Channel Modeling for Vehicle-to-Vehicle Communications at 5.9 GHz,"*IEEE Antennas and Propagation Society International Symposium*, 2008.

[22] G. P. Grau, D. Pusceddu, S. Rea, O. Brickley, M. Koubek, D. Pesch,"Vehicle-2-vehicle communication channel evaluation using the CVIS platform,"*IEEE Communication Systems Networks and Digital Signal Processing (CSNDSP) symposium*, July, 2010.

[23] J.R. Gallardo, D. Makrakis, H.T. Mouftah,"Performance Analysis of the EDCA Medium Access Mechanism over the Control Channel of an IEEE 802.11p WAVE Vehicular Network," *Communications, 2009. ICC '09. IEEE International Conference on*, pp.1-6,14-18 June, 2009.

[24] S. Chang, J. Cha, S. Lee, "Adaptive EDCA mechanism for vehicular ad-hoc network,"*Information Networking (ICOIN), 2012 International Conference on*, pp.379,383, 1-3 Feb. 2012.

[25] S. Grafling, P. Mahonen, J. Riihijarvi, "Performance evaluation of IEEE 1609 WAVE and IEEE 802.11p for vehicular communications,"*Ubiquitous and Future Networks (ICUFN), 2010 Second International Conference on* , pp.344-348, 16-18 June 2010.

[26] A.J. Ghandour, M. Di Felice, L. Bononi, and H. Artail, "Modeling and simulation of WAVE 1609.4-based multi-channel vehicular ad hoc networks,"*In Proceedings of the 5th International ICST Conference on Simulation Tools and Techniques (SIMUTOOLS '12). ICST (Institute for Computer Sciences, Social-Informatics and Telecommunications Engineering)*, ICST, Brussels, Belgium, 148-156, 2012.

[27] "OPNET Modeler Network Simulation" in *http://www.opnet.com/products/opnet-products.html*.

[28] V. Shivaldova, A. Paier, D. Smely, C.F. Mecklenbrauker, "On roadside unit antenna measurements for vehicle-to-infrastructure communications,"*Personal Indoor and Mobile Radio Communications (PIMRC), 2012 IEEE 23rd International Symposium on* , pp.1295,1299, 9-12 Sept. 2012.

[29] J. Maurer, T. Fugen, and W. Wiesbeck, "Narrow-band measurement and analysis of the inter-vehicle transmission channel at 5.2 GHz," *IEEE 55th Vehicular Techn. Conf.*, pp. 1274 - 1278, 2002.

[30] A.F. Molisch, F. Tufvesson, J. Karedal, C. Mecklenbrauker, "Propagation aspects of vehicle-to-vehicle communications - an overview," *IEEE Radio and Wireless Symposium*, pp.179 - 182, 18-22 Jan. 2009.

[31] M.K. Simon, Mohamed-Slim Alouini, "Digital communications over fading channel," John Wiley and Sons, Inc., New York, 2000.

[32] A. S. Akki and F. Haber, "A statistical model for mobile-to-mobile land communication channel," *in IEEE Trans. on Veh. Technol.*, vol. VT-35, no. 1, Feb. 1986.

[33] C.S. Patel, G.L. Stuber, and T.G. Pratt, "Simulation of Rayleigh-Faded Mobile-to-Mobile Communication Channels," *IEEE Transactions on Communications*, vol.53, no.10, pp.1773, Oct. 2005.

[34] N. C. Beaulieu and C. Cheng, "An Efficient Procedure for Nakagami-m Fading Simulation," in *Proc. of IEEE Globecom 2001*, volume 6, pp.3336âĂŞ3342, Nov 2001.

[35] M. Nakagami, "The m-distribution, a general formula of intensity distribution of rapid fading," in *Statistical methods in radio wave propagation*, W. G. Hoffman, Ed, Oxford, UK: Pergamon, 1960.

[36] W. H. Press, S. A. Teukolsky, W.T.Vetterling, B.P. Flannery, "Numerical Recipes: The Art of Scientific Computing", 3rd ed, Cambridge University Press, New York, 2007.

[37] H. Chong, M. Dianati, R. Tafazolli, R. Kernchen, X. Shen, "Analytical Study of the IEEE 802.11p MAC Sublayer in Vehicular Networks," in *Intelligent Transportation Systems, IEEE Transactions on*, vol.13, no.2, pp.873,886, June 2012.

[38] F.J . Martinez, Toh Chai-Keong Toh, J.-C. Cano, C.T. Calafate, P. Manzoni, "Realistic Radio Propagation Models (RPMs) for VANET Simulations," in IEEE *Wireless Communications and Networking Conference*, 2009, pp.1-6, 5-8 April 2009.

[39] M. Torrent-Moreno, "Inter-vehicle communications: assessing information dissemination under safety constraints," in *IEEE Fourth Annual Conference on Wireless on Demand Network Systems and Services*, pp.59-64, 24-26 Jan. 2007.

[40] M. Killat, F. Schmidt-Eisenlohr, H. Hartenstein, C. RÃűssel, P. Vortisch, S. Assenmacher, and F. Busch, "Enabling efficient and accurate large scale simulations of VANETs for vehicular traffic management," in *Proceedings of the fourth ACM international workshop on Vehicular ad hoc networks (VANET '07)*, pp.29-38, 2007.

[41] Q. Xu, T. Mak, J. Ko, and R. Sengupta, "Vehicle-to-vehicle safety messaging in DSRC," in *Proceedings of the 1st ACM international workshop on Vehicular ad hoc networks (VANET '04)*, pp.19-28, 2004.

[42] Y. Zang, L. Stibor, G. Orfanos, S. Guo, and H-J. Reumerman, "An error model for inter-vehicle communications in highway scenarios at 5.9 GHz," in *Proceedings of the 2nd ACM international workshop on Performance evaluation of wireless ad hoc, sensor, and ubiquitous networks (PE-WASUN '05)*, pp.49-56, 2005.

[43] C. Sommer, S. Joerer, F. Dressler, "On the applicability of two-ray path loss models for vehicular network simulation," in *IEEE Vehicular Networking Conference (VNC)*, pp.64-69, 14-16 Nov. 2012.

[44] C. Sommer, D. Eckhoff, R. German, F. Dressler, "A computationally inexpensive empirical model of IEEE 802.11p radio shadowing in urban environments," in *IEEE Eighth International Conference on Wireless On-Demand Network Systems and Services (WONS)*, pp.84-90, 26-28 Jan. 2011.

Acronyms

List of Acronyms

ITS Intelligent Transportation Systems

WAVE Wireless Access in Vehicular Environments

RSU Road Side Unit

OBU On Board Unit

V2I Vehicle to Infrastructure

V2V Vehicle to Vehicle

PHY Physical Layer

CSMA/CA Carrier Sense Multiple Access Collision Avoidance

MAC Medium Access Control

DSRC Dedicated Short Range Communications

BSS Basic Service Set

AP Access Point

OSI Open System Interconnect

ETSI European Telecommunications Standards Institute

ACR Adjacent Channel Rejection

SEM Spectrum Emission Mask

LAN Local Area Network

QoS Quality of Service

WLAN Wireless Local Area Network

EDCA Enhanced Distributed Channel Access

AIFS Arbitration Inter-frame Space

AC Access Categories

CW Contention Window

TXOP Transmit Opportunity

MPDU MAC Protocol Data Unit

CCHI Control Channel Interval

SCHI Service Channel Interval

OFDM Orthogonal Frequency Division Multiplexing

DES Discrete Event Simulation

LTE Long-Term Evolution

UMTS Universal Mobile Telecommunications System

HTTP Hypertext Transfer Protocol

AODV Ad-Hoc On Demand Distance Vector routing

DSR Dynamic Source Routing

GRP Geographic Routing Protocol

OLSR Optimized Link State Routing

PCF Point Coordination Function

DCF Distributed Coordination Function

TNO Netherlands Organization for Applied Scientific Research

BER Bit Error Rate

SNR Signal to Noise Ratio

RWM Random Waypoint Model

ToS Type of Service

QPSK Quadrature Phase Shift Keying

QAM Quadrature Amplitude Modulation

NF Noise Figure

SIFS Short Inter Frame Spacing

DIFS DCF Interframe Space

WLANS Wireless Local Area Network Server

WLANW Wireless Local Area Network Workstation

BPSK Binary Phase Shift Keying

LoS Line of Sight

DSPL Dual Slope Piecewise Linear

SINR Signal to Interference and Noise Ratio

WSSUS Wide Sense Stationary Uniform Scattering

FFT Fast Fourier Transform

PDF Probability Density Function

WSS Wide Sense Stationary

TMM Terrain Modeling Module

PER Packet Error Rate

OS Operating System

MSVS Microsoft Visual Studio

CEC Commission of European Communities

WARP2 Wireless Access Radio Protocol 2